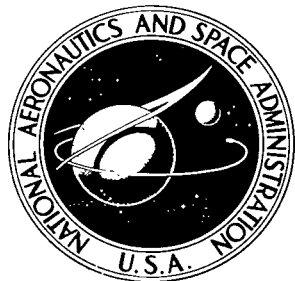


NASA TN D-5843

NASA TECHNICAL NOTE



NASA TN D-5843

C. I

LOAN COPY: EDITION
ALBUQUERQUE (WCOL)
KIRKLAND AFB, NM
032586

010



TECH LIBRARY KAFB, NM

EXPERIMENTAL INVESTIGATION OF AN ATTITUDE CONTROL SYSTEM THAT USES STAR TRACKERS AND INERTIA WHEELS

by Robert D. Showman and Bruce H. Dishman

Ames Research Center

Moffett Field, Calif. 94035



NATIONAL AERONAUTICS AND SPACE ADMINISTRATION • WASHINGTON, D. C. • JUNE 1970



0132586

1. Report No. NASA TN D-5843	2. Government Accession No.	3. Recipient's Catalog No.	
4. Title and Subtitle EXPERIMENTAL INVESTIGATION OF AN ATTITUDE CONTROL SYSTEM THAT USES STAR TRACKERS AND INERTIA WHEELS	5. Report Date June 1970	6. Performing Organization Code	
7. Author(s) Robert D. Showman and Bruce H. Dishman	8. Performing Organization Report No. A-3515	10. Work Unit No. 125-19-03-06-00-21	
9. Performing Organization Name and Address NASA Ames Research Center Moffett Field, Calif., 94035	11. Contract or Grant No.	13. Type of Report and Period Covered Technical Note	
12. Sponsoring Agency Name and Address National Aeronautics and Space Administration Washington, D.C. 20546	14. Sponsoring Agency Code		
15. Supplementary Notes			
16. Abstract Three methods of processing star tracker gimbal angle measurements to derive attitude control signals for a satellite were simulated with spacecraft-type hardware. Each method is a simplification of the exact kinematic equations relating the star tracker gimbal angle rates to the satellite angular rates. An analytic analysis has shown a system that uses any one of the three methods is stable for small deviations about the commanded attitude.			
17. Key Words (Suggested by Author(s)) Control system Star trackers Simulation	18. Distribution Statement Unclassified-Unlimited STAR Category - 31		
19. Security Classif. (of this report) Unclassified	20. Security Classif. (of this page) Unclassified	21. No. of Pages 39	22. Price* \$3.00



TABLE OF CONTENTS

	<u>Page</u>
SYMBOLS	iv
SUMMARY	1
INTRODUCTION	1
ATTITUDE CONTROL SIGNALS OBTAINED FROM STAR TRACKERS	3
Indeterminant Condition	6
Effect of an Error in Measuring the Gimbal Angle	7
Effect of Multiple Equilibrium Points on System Behavior	7
RESULTS OF SIMULATION	9
Small Angle Results	9
Transient response	10
Steady-state behavior	12
Large Angle Results	14
Large angle slue	14
System behavior near the restricted region	14
CONCLUSIONS	17
APPENDIX - SIMULATION EQUIPMENT	18
REFERENCE	20
FIGURES	21

SYMBOLS

$1^V, 2^V, 3^V$	orthonormal coordinate system defining control axes of table
$1^i, 2^i, 3^i$	orthonormal coordinate system for the i th star tracker
$c\gamma_i$	cosine γ_i
d_{12}	constant gain for the partial processor
$d(\cdot)$	differential of (\cdot)
I_1, I_2, I_3	table inertia about the control axes
K_c	gain of the compensator
K_m	gain of the motor
M_c	constant processor
M_I	ideal processor
M_p	partial processor
N	geometry matrix
S_{ij}	gains for the constant processor
$s\gamma_1$	$\sin \gamma_1$
$t\beta_1$	$\tan \beta_1$
V_ϕ, V_θ, V_ψ	roll, pitch, and yaw motor voltages
$WR1, WR2, WR3$	roll, pitch, and yaw wheel speeds
$\alpha_i, \beta_i, \gamma_i$	rotations about the 1, 2, and 3 axes of the i th star tracker
$\beta_{1c}, \gamma_{1c}, \beta_{2c}$	commanded star tracker gimbal angles
$\beta_{10}, \gamma_{10}, \beta_{20}, \gamma_{20}$	initial star tracker gimbal angles
δ	angle between the stars
$\Delta\alpha_i, \Delta\beta_i, \Delta\gamma_i$	first-order approximation to rotation about the 1, 2, and 3 axes of the i th star tracker
$\Delta\phi, \Delta\theta, \Delta\psi$	first-order approximation to rotation about the control axes

ϕ, θ, ψ	roll, pitch, and yaw Euler angles. The Euler angle sequence used for this study is yaw, roll, and pitch.
$\dot{\phi}, \dot{\theta}, \dot{\psi}$	roll, pitch, and yaw Euler angle rates
$\varepsilon_\phi, \varepsilon_\theta, \varepsilon_\psi$	control signals obtained from the processors
τ_1, τ_2	compensator time constant
τ_L	lag filter time constant
τ_M	motor time constant
$\omega_{1V}, \omega_{2V}, \omega_{3V}$	inertial angular rate of the table

EXPERIMENTAL INVESTIGATION OF AN ATTITUDE CONTROL SYSTEM

THAT USES STAR TRACKERS AND INERTIA WHEELS

Robert D. Showman and Bruce H. Dishman

Ames Research Center

SUMMARY

Three methods of processing star tracker gimbal angle measurements to derive attitude control signals for a satellite were simulated with actual spacecraft type hardware. Each method is a simplification of the exact kinematic equations relating the star tracker gimbal angle rates to the satellite angular rates. The first method, called the ideal processor, is a direct mechanization of the first-order approximation to the exact kinematic equations. The other two methods, called the partial and constant processors, are variations of the ideal processor that simplify the mechanization. The analysis in NASA TN D-4490 showed that a system that uses any one of the three processors is stable for small deviations about the commanded attitude.

The attitude control system consisted of an air-bearing table to simulate the satellite, gimbaled star trackers for attitude information, motor-inertia-wheel combinations to change the satellite's attitude, and simulated stars as targets for the star trackers. An on-line digital computer performs as a real time controller by converting the star tracker gimbal angle measurements into attitude control signals.

The results of the simulation showed that (1) with each processor the system performed as predicted; (2) initial momentum could affect the transient behavior; (3) noise, not necessarily generated in the processor, could decrease the steady-state pointing accuracy; (4) an error in the gimbal angle measurements caused the equilibrium point to vary; that is, the system stabilized but not at the desired inertial attitude; (5) the system using the partial processor stabilized the table for reorientations as large as 55°; and (6) although the satellite cannot be stabilized in the restricted region where the attitude is undefined, the system with the partial processor might maneuver the satellite through the region.

INTRODUCTION

Three methods of processing star tracker gimbal angle measurements to obtain satellite attitude control signals were investigated in reference 1. The methods were derived by approximating the exact kinematic equations relating the star tracker gimbal angle rates to the satellite body rates. Each method had to be simple enough so that a computer would not be required for the mechanization. The three methods were designated the "ideal," "partial," and "constant" processors. The ideal processor is a direct mechanization of

the first-order terms of the exact kinematic equations. The other two are variations of the ideal processor that further simplify the mechanization. The analysis (ref. 1) used a simplified representation for both the dynamics and kinematics to investigate the behavior of a system such as the OAO with each processor. The results of this analysis showed that the system would perform satisfactorily in the region where the approximations are valid.

This paper presents the results of a simulation with spacecraft type hardware of an attitude control system using each of the processors. The purpose of the investigation is to determine the effect of the approximations used in the analytic study. First, the small angle motion of the system was investigated to determine the effect of simplifying the dynamics in the analytic study. Simulating the small angle motion will confirm the results of the analytic study. Second, it was desired to investigate the large angle motion to determine the effect of simplifying the kinematics in the analytic study. Simulating the large angle motion will indicate the magnitude of angular reorientations through which the partial processor can control the satellite.

The Ames Satellite Attitude Control Simulator (SACS) and a digital and an analog computer were used to simulate the control system (fig. 1). The SACS (fig. 2) includes an air bearing table that simulates the satellite. On it are mounted two gimballed star trackers for providing the position information and three reaction wheels for providing the control torques (fig. 3). Simulated stars are also provided as targets for the star trackers (fig. 2). Star tracker gimbal angle measurements from the table are transmitted directly to a digital computer where each of the processor is mechanized (fig. 1). After the gimbal angle measurements pass through a processor, the control signals from the digital computer are passed through a passive lead network mechanized on an analog computer. The signals from the lead network are limited before being returned to the SACS as excitation signals to the reaction wheels. (A more complete description of the SACS is given in the appendix.)

The first section of the paper reviews the derivation of the attitude control signals from the star tracker gimbal angle measurements and discusses three characteristics of the processors. First, the indeterminant condition that can result from using the processors is reviewed. Second, the effect of an error in measuring the star tracker gimbal angles is investigated. Third, the effect of multiple equilibrium points on the behavior of the system for large angle motion is discussed. The last section is devoted to the results of the simulation. The small angle and large angle results are presented separately. The small angle maneuvers considered are less than or equal to 5° . Both the transient and steady-state behavior of the system using each processor are examined. The large angle section discusses the use of the partial processor to control the satellite for large angle reorientations. The use of the partial processor to control the satellite near and through the restricted region is also discussed.

ATTITUDE CONTROL SIGNALS OBTAINED FROM STAR TRACKERS

The star tracker provides the position information necessary to control the attitude of the table. The control signals are obtained by appropriately processing the gimbal angle measurements and are used to provide the excitation for the reaction wheels. The present section reviews the three processors and the indeterminant condition that can result from using them (ref. 1). In addition, both the effect of errors in measuring the gimbal angles and of multiple equilibrium points on the behavior of the system are described.

The mounting arrangement of the star trackers with respect to the control axes of the table for this study (1^V - roll, 2^V - pitch, 3^V - yaw) is shown in figure 4. The trackers are shown with their gimbal angles at null. The outer gimbal axes are labeled 1, 2, and 3 with a superscript indicating the tracker number; thus, 2^1 denotes the inner axis of tracker number 1.

The processors were derived in reference 1 by approximating the exact kinematic rate equations relating tracker gimbal angle rates to vehicle angular rates.¹ These linearized equations relating the gimbal angle errors to the satellite attitude errors are

$$\begin{bmatrix} \Delta\beta_1 \\ \Delta\gamma_1 \\ \Delta\beta_2 \end{bmatrix} = N \begin{bmatrix} \Delta\phi \\ \Delta\theta \\ \Delta\psi \end{bmatrix} \quad (1)$$

where

$$N = \begin{bmatrix} 0 & s\gamma_1 & c\gamma_1 \\ 1 & -c\gamma_1 t\beta_1 & s\gamma_1 t\beta_1 \\ 0 & c\gamma_2 & -s\gamma_2 \end{bmatrix}$$

The error in the table's attitude can now be estimated from the gimbal angle measurements, if they are independent, by solving equation (1). The first processor, called the ideal processor, is defined as the first-order approximation relating the vehicle control signals to the gimbal angle errors and is

¹Tracker 1 in this report corresponds to tracker 1 in the reference. The rate equations for tracker 2 in this report can be derived in the manner described in the appendix of the reference by letting

$$P = \begin{bmatrix} 0 & 0 & -1 \\ 0 & 1 & 0 \\ 1 & 0 & 0 \end{bmatrix}$$

$$\begin{bmatrix} \varepsilon_\phi \\ \varepsilon_\theta \\ \varepsilon_\psi \end{bmatrix} = M_I \begin{bmatrix} \Delta\beta_1 \\ \Delta\gamma_1 \\ \Delta\beta_2 \end{bmatrix}$$

where

$$M_I = \frac{1}{c(\gamma_1 - \gamma_2)} \begin{bmatrix} -s(\gamma_1 - \gamma_2)t\beta_1 & c(\gamma_1 - \gamma_2) & t\beta_1 \\ s\gamma_2 & 0 & c\gamma_1 \\ c\gamma_2 & 0 & -s\gamma_1 \end{bmatrix} \quad \left. \right\} (2)$$

and

$$[\varepsilon_\phi \quad \varepsilon_\theta \quad \varepsilon_\psi] = [\Delta\phi \quad \Delta\theta \quad \Delta\psi]$$

for the ideal processor only. Since the outer gimbal axes of the paired trackers are parallel and two inner and one outer gimbal error is used, equation (2) is the simplest ideal processor to mechanize (ref. 1). Its mechanization insures that, to a first order, the control signals (ε_ϕ , ε_θ , ε_ψ) are decoupled; that is, $M_I N = I$ where I is the identity matrix.

Simpler forms to mechanize are obtained from approximations to the ideal processor. If the more complex terms are made constant and only the simple sine and cosine terms are mechanized, the transformation of equation (2) becomes

$$M_p = \begin{bmatrix} 0 & 1 & 0 \\ d_{12}s\gamma_2 & 0 & d_{12}c\gamma_1 \\ d_{12}c\gamma_2 & 0 & -d_{12}s\gamma_1 \end{bmatrix} \quad (3)$$

where M_p is designated as the partial processor. The constants for the 11 and 13 elements do not influence the stability of the system because the outer gimbal axes are parallel and two inner and one outer gimbal angle error is used. They are therefore equated to zero. The term $1/C(\gamma_1 - \gamma_2)$ in equation (2) is represented by d_{12} which is constant for all commands and is not evaluated at each set of command angles. The product of the partial processor and the linearized equations for the star tracker dynamics (eq. (1)) is

$$\begin{bmatrix} \varepsilon_\phi \\ \varepsilon_\theta \\ \varepsilon_\psi \end{bmatrix} = \begin{bmatrix} 1 & -c\gamma_1t\beta_1 & s\gamma_1t\beta_1 \\ 0 & d_{12}c(\gamma_1 - \gamma_2) & 0 \\ 0 & 0 & d_{12}c(\gamma_1 - \gamma_2) \end{bmatrix} \begin{bmatrix} \Delta\phi \\ \Delta\theta \\ \Delta\psi \end{bmatrix} \quad (4)$$

It follows from equation (4) that the partial processor insures the independence of two control channels (ϵ_0 , ϵ_ψ) rather than all three as does with the ideal processor. Also, the gains of the pitch and yaw channels are functions of the outer gimbal angles, whereas their gains were constant with the ideal processor.

Another approximation to the ideal processor, designated the "constant processor," allows even simpler mechanization than the partial processor. The constant processor is obtained by letting each of the nonzero elements of the ideal processor be constant. The elements of the matrix then are not parameters to be evaluated at each set of commanded gimbal angles but are to remain constant at least in magnitude over the complete range of allowed commanded angles. The constant processor is

$$M_C = \begin{bmatrix} 0 & 1 & 0 \\ S_{21} & 0 & S_{23} \\ S_{31} & 0 & S_{33} \end{bmatrix} \quad (5)$$

where the constants for the 11 and the 13 elements are again equated to zero since they do not influence stability. The product matrix $M_C N$ is

$$\begin{bmatrix} \dot{\phi} \\ \epsilon_0 \\ \epsilon_\psi \end{bmatrix} = \begin{bmatrix} 1 & -c\gamma_1 t\beta_1 & s\gamma_1 t\beta_1 \\ 0 & (S_{21}s\gamma_1 + S_{23}c\gamma_2) & (S_{21}c\gamma_1 - S_{23}s\gamma_2) \\ 0 & (S_{31}s\gamma_1 + S_{33}c\gamma_2) & (S_{31}c\gamma_1 - S_{33}s\gamma_2) \end{bmatrix} \begin{bmatrix} \Delta\phi \\ \Delta\theta \\ \Delta\psi \end{bmatrix} \quad (6)$$

Equation (6) shows that the pitch and yaw error signals are independent of the motion about the roll axis. However, the pitch and yaw signals are crosscoupled and both signals are coupled into roll.

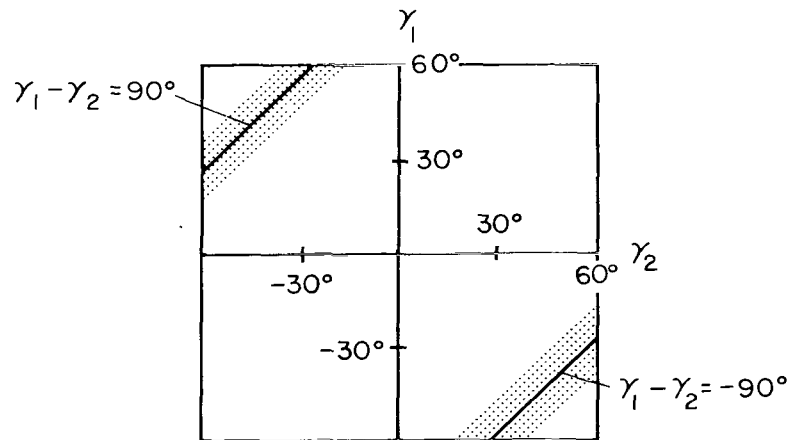
The stability of the system (fig. 5) using each of the three processors was also investigated in reference 1. The analysis assumed the following conditions: (1) The mass distribution of the vehicle is such that the moments of inertia about any three orthogonal axes are equal; (2) gyroscopic coupling due to inertia wheel rotation is negligible; (3) linearized equations validly describe the motor-inertia-wheel combination; (4) the motor torque is limited and the saturation type nonlinearity is validly represented by a describing function for a stability analysis; (5) the star trackers track perfectly; (6) the star trackers and reaction wheels are perfectly aligned with the control axis; (7) linearized equations validly describe the gimbal angle errors ($\Delta\beta_1$, $\Delta\gamma_1$, $\Delta\beta_2$) as a function of the satellite's deviation from its nominal ($\Delta\phi$, $\Delta\theta$, $\Delta\psi$); (8) the linearization of the Euler angle rate equations is valid; (9) no external torques exist; and (10) the elements of the processors are constants evaluated at each set of command angles.

The analysis results showed that the system using either the ideal or partial processor was stable and provided the desired performance for any set

of commanded gimbal angles; that is, the system is stable for small deviations about any physically possible set of commanded angles. The system using the constant processor was also stable and provided the desired performance for small deviations about any set of commanded gimbal angles. The range of commanded gimbal angles is $\pm 60^\circ$. Although the system performed as desired, the following three characteristics should be considered: (1) the indeterminant condition, (2) the effect of an error in measuring the gimbal angles, and (3) the effect of multiple equilibrium points.

Indeterminant Condition

The first characteristic to be considered is the processor's inability to estimate the attitude of the satellite under certain conditions. Each processor provides an estimate of the satellite's attitude error if the gimbal angle errors are independent. However, the gimbal angle errors become dependent when the determinant of equation (1) vanishes (i.e., when $c(\gamma_1 - \gamma_2) = 0$) and an indeterminant condition exists. The three-dimensional error measured about the control axes ($\Delta\phi$, $\Delta\theta$, $\Delta\psi$) then maps into three coplanar gimbal errors ($\Delta\beta_1$, $\Delta\gamma_1$, $\Delta\beta_2$). Under these circumstances, the satellite attitude error cannot be determined from the gimbal angle measurements. A physical interpretation indicates that the indeterminant condition occurs when the plane formed by the lines of sight to the two stars includes the outer gimbal axes of the star trackers, or, equivalently, the roll axis of the vehicle. According to figure 6, the condition occurs when the plane formed by the lines of sight to stars A and B contains point c which lies along the roll axis. Since the attitude of the satellite cannot be determined from the gimbal angle measurements, a region about the indeterminant condition must be established in which operation must be restricted. From the analytic study, the proposed restricted region is $80^\circ < |\gamma_{1c} - \gamma_{2c}| < 100^\circ$, shown as the shaded region in sketch (a).



Sketch (a)

Effect of an Error in Measuring the Gimbal Angles

The second characteristic to be considered is an inaccurate measurement of the star tracker gimbal angles which causes the equilibrium position of the satellite to vary. An estimate of the effect of the error in gimbal angle measurement on the equilibrium position is given by taking the total differential of equation (2):

$$\begin{bmatrix} d(\Delta\phi) \\ d(\Delta\theta) \\ d(\Delta\psi) \end{bmatrix} = \begin{bmatrix} -t(\gamma_1 - \gamma_2)t\beta_1 & 1 & t\beta_1/c(\gamma_1 - \gamma_2) \\ s\gamma_2/c(\gamma_1 - \gamma_2) & 0 & c\gamma_1/c(\gamma_1 - \gamma_2) \\ c\gamma_2/c(\gamma_1 - \gamma_2) & 0 & -s\gamma_1/c(\gamma_1 - \gamma_2) \end{bmatrix} \begin{bmatrix} d(\Delta\beta_1) \\ d(\Delta\gamma_1) \\ d(\Delta\beta_2) \end{bmatrix} \quad (7)$$

where

$$\Delta\beta_1 = \beta_1 - \beta_{1c}$$

$$\Delta\beta_2 = \beta_2 - \beta_{2c}$$

$$\Delta\gamma_1 = \gamma_1 - \gamma_{1c}$$

If the system is at the desired position, the gimbal angles are equal to their commanded values; that is, $\Delta\beta_1$, $\Delta\gamma_1$ and $\Delta\beta_2$ are zero implying $\Delta\phi$, $\Delta\theta$, and $\Delta\psi$ are zero. Assume that an inaccurate measurement of the outer gimbal angle γ_1 occurs. The angle $d(\Delta\gamma_1)$ becomes nonzero. The variation in $d(\Delta\gamma_1)$ results in an equal change in the equilibrium point about the roll axis $d(\Delta\phi)$. Now consider an error in measuring either of the inner gimbal angles; that is, $d(\Delta\beta_1)$ and $d(\Delta\beta_2)$ are nonzero. These inaccurate measurements result in a variation of the equilibrium point in all three axes ($d(\Delta\phi)$, $d(\Delta\theta)$, $d(\Delta\psi)$). If the difference between the outer gimbal angles is about zero ($c(\gamma_1 - \gamma_2) \rightarrow 1$), then the variation in the equilibrium position is approximately equal to the variation in the inner gimbal angles. However, if the system is operating near the restricted region ($|\gamma_1 - \gamma_2| \rightarrow 90^\circ \Rightarrow c(\gamma_1 - \gamma_2) \rightarrow 0$), the change in the equilibrium position is much larger than the variation in inner gimbal angle. For example, if $(\gamma_1 - \gamma_2) = 80^\circ$ and $\beta_1 = 60^\circ$, the change in the equilibrium position about the roll axis is about 10 times the variation in the inner gimbal angles. Therefore, if the system is to operate near the indeterminate condition, the gimbal angle measurements must be accurate. If the gimbal measurements are inaccurate, the system will, in general, stabilize but not at the desired inertial attitude. The effect of inaccurate gimbal angle measurements on the behavior of the system was observed during the simulation. For example, with the system stabilized at a specific set of commanded angles, the attitude of the table varied, in one instance, approximately 2° in yaw.

Effect of Multiple Equilibrium Points on System Behavior

The last characteristic to be considered is the multiple equilibrium points. Each set of commanded star tracker gimbal angles has two equilibrium points because only three of the four gimbal angles of the paired star

trackers are commanded. Since the trackers are pointing at known guide stars, the angle between the stars can be determined. The magnitude of the fourth gimbal angle at the commanded position can then be determined from the three commanded angles and the angle between the stars. For example, the angle between the stars δ can be written as a function of the gimbal angles as

$$\cos \delta = \sin \beta_1 \sin \beta_2 - \cos \beta_1 \cos \beta_2 \sin(\gamma_1 - \gamma_2) \quad (8)$$

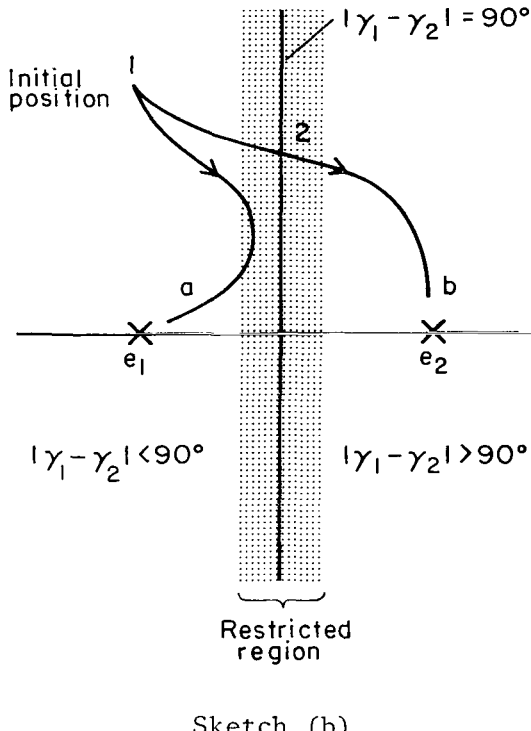
Since the four known angles are $\delta = \delta_0$, $\beta_1 = \beta_{1c}$, $\gamma_1 = \gamma_{1c}$ and $\beta_2 = \beta_{2c}$, the fourth gimbal angle is

$$\sin(\gamma_{1c} - \gamma_2) = \frac{-\cos \delta_0 + \sin \beta_{1c} \sin \beta_{2c}}{\cos \beta_{1c} \cos \beta_{2c}} \quad (9)$$

If $\sin(\gamma_{1c} - \gamma_2) > 0$, then $(\gamma_{1c} - \gamma_2)$ can be either in the first or second quadrant. If $\sin(\gamma_{1c} - \gamma_2) < 0$, then $(\gamma_{1c} - \gamma_2)$ can be either in the third or fourth quadrant. Since the indeterminant condition occurs when $|\gamma_{1c} - \gamma_2| = 90^\circ$, the two solutions correspond to equilibrium points (e_1 , e_2 in sketch (b)) on opposite sides of the indeterminant condition.

The effect of multiple equilibria on the behavior of the system is now investigated. For the system using the partial processor to be stable, reference 1 showed that

$$d_{12} \gtrless 0 \quad \text{if} \quad c(\gamma_{1c} - \gamma_{2c}) \gtrless 0 \rightarrow |\gamma_{1c} - \gamma_{2c}| \lesssim 90^\circ$$



Thus, if $d_{12} > 0$, e_1 and e_2 are a stable and an unstable equilibrium point, respectively. Conversely, if $d_{12} < 0$, then e_1 and e_2 are an unstable and a stable equilibrium point.

The sign of d_{12} must be controlled as a function of the commanded outer gimbal angles and not the actual outer gimbal angles. If the sign of d_{12} is controlled as a function of the actual gimbal angles, the system could stabilize at the incorrect equilibrium position. For example, assume it is desired to drive the system from point "1" to e_1 (sketch (b)). Therefore, $d_{12} > 0$ so that e_1 is a stable equilibrium point. If the system responds as shown in the sketch (trajectory (b)) and d_{12} is controlled as a function of the actual outer gimbal angles, the sign of d_{12} changes at point 2. The equilibrium point e_2 then becomes a stable equilibrium. The system now could drive to e_2 . However, if the

sign of d_{12} is controlled as a function of the commanded angles, the sign of d_{12} does not change at point 2 and e_1 is always the stable equilibrium point.

The multiple equilibrium points do not affect the results of the analytic study (ref. 1) because only small changes in attitude were considered. Since the initial and commanded angles must be outside the restricted region, the angle between the two equilibrium points is at least 20° (assuming the restricted region is $80^\circ < |\gamma_1 - \gamma_2| < 100^\circ$). It was also assumed that, if the system might penetrate the restricted region, a new set of guide stars would be chosen. However, the effect of multiple equilibrium points must now be considered since larger angle motions are being investigated.

RESULTS OF THE SIMULATION

The results of the simulation will be presented separately for small angle and large angle commands. The small angle section discusses the behavior of the system using each of the three processors for reorientations no larger than 5° . The section begins with a comparison of the analytic model with the simulator. Then the transient and steady-state behavior of the system using each of the three processors are discussed.

The large angle section describes the behavior of the system using only the partial processor for angular reorientations of the table as large as 55° . First, the simulation results for the large angle maneuvers are presented. Finally, the behavior of the system when entering and passing through the restricted region is investigated.

Small Angle Results

The small angle results of the hardware simulation are presented to verify the analytic study and to show the applicability of the processors to a real system. The simulation presents the system with a more severe environment than the real system would encounter. If the system performs satisfactorily for the simulation, it is expected that it would perform adequately for the real situation. The simulation and analytic results might differ because of the following differences between the analytic model and the simulator: (1) The inertias about the control axes are not equal. Also, the products of inertia were nonzero but small; (2) the gyroscopic coupling torques are not necessarily negligible. However, the simulator approximates the analytic model if the system angular momentum is identically zero; (3) both static friction and deadzone exist in the motor; (4) the star trackers cannot ideally track the stars. The ability of the trackers to point at the star depends on the table angular rate. For small deviations, the rates are small and the lag introduced by the trackers is small; (5) external torques are ever present in the simulation but were not considered in the analytic study. The magnitude of the torque varied from run to run; (6) the trigonometric elements of the ideal and partial processors are no longer constants evaluated at the command

angles, but are evaluated at the present gimbal angle. For small angular changes, the variation of the constants would be small.

Transient response- The transient response of the system using each processor is investigated. First, the behavior of the system for an initial attitude error about a single control axis is examined. Next, a typical multiple axis maneuver using each processor is shown. Finally, the effect of initial momentum on the transient behavior is discussed.

The response of the system to an attitude error about a single control axis was made to investigate the coupling introduced by the processor. Each run was made with zero initial momentum. If the external torques are negligible, the system momentum remains small. Thus, the gyroscopic and inertia coupling torques are negligible. The only coupling would then result from either an inexact estimate of the error from the linearized equations as occurs with the ideal processor or from an incomplete processing of the gimbal angle information, such as occurs with the partial and constant processor.

The response of the system with each processor is shown in figures 7, 8, and 9. Each figure shows the time histories of the linearized Euler angles ($\Delta\phi$, $\Delta\theta$, $\Delta\psi$) (i.e., the output of the ideal processor) of three separate runs labeled (a), (b), and (c). Each run has an initial attitude error of 5° about a single control axis; that is, runs (a), (b), and (c) have an initial error of 5° about the roll, pitch, and yaw axes, respectively. The commanded and initial gimbal angles for the runs shown in the three figures are given in table 1. Also shown are the time constants for the compensation networks and the gains for the system. The difference between the commanded outer gimbal angles ($\gamma_{1c} - \gamma_{2c} = -15.2$) indicates the runs were not made near the restricted region.

TABLE 1.- DATA FOR FIGURES 7, 8, AND 9

	β_1	γ_1	β_2	γ_2
Command angles	27.3	26.7	6.8	41.9
a	27.3	31.8	6.8	45.9
b	29.3	24.2	10.5	41.5
c	31.6	28.0	3.6	41.4

$$d_{12} = 5.77 ; \quad S_{21} = 0 ; \quad S_{23} = 4.25 ; \quad S_{31} = 2.0 ; \quad S_{33} = -3.5$$

$$\tau_1 = 4.55 ; \quad \tau_2 = 0.455 ; \quad K_C = 4700 ; \quad \tau_L = 0.22$$

The response of the system using the ideal processor is shown in figure 7. The transient responses show that no detectable coupling is introduced between control channels when the ideal processor is used for reorientations of 5° .

The response of the system using the partial processor is shown in figure 8. The three runs show the following: (a) roll motion is not coupled into either pitch or yaw; (b) pitch motion is coupled only into roll; and (c) yaw motion is coupled only into roll. The coupling of pitch and yaw

motion into roll is predicted by the analytic model (eq. (4)) if the gimbal angles of tracker number 1 (β_1 , γ_1) are nonzero. The analytic model indicates no coupling should occur between control channels if $\beta_1 = 0$. To verify the analytic study further, a set of runs similar to those in figure 8 was made with $\beta_{1c} = 0$. The responses showed that no detectable coupling occurs between the control channels. The response curves were very similar to those shown in figure 7 for the ideal processor.

The response of the system using the constant processor is shown in figure 9. The constants for the processor are given in table 1. If evaluated at the specified constants and the commanded gimbal angles, the analytic model (eq. (6)) becomes

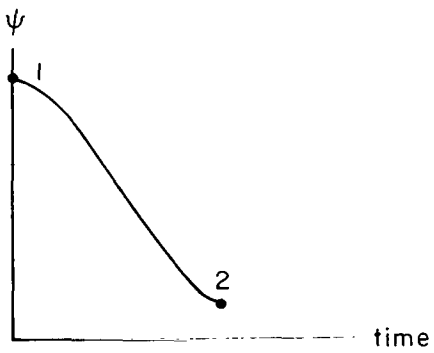
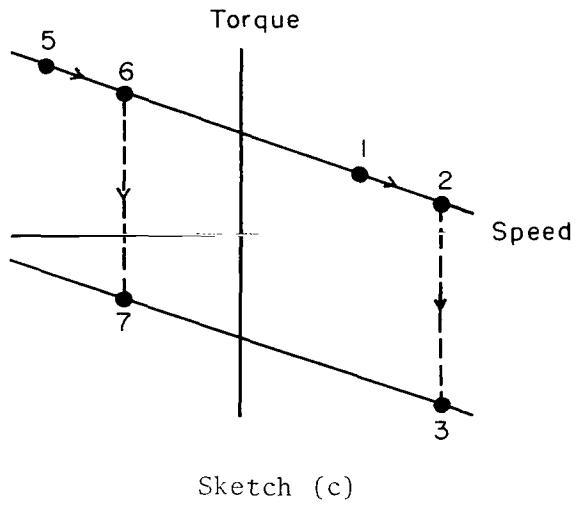
$$\begin{bmatrix} \varepsilon_\phi \\ \varepsilon_\theta \\ \varepsilon_\psi \end{bmatrix} = \begin{bmatrix} 1 & -0.461 & 0.232 \\ 0 & 3.165 & -2.836 \\ 0 & -1.709 & 4.123 \end{bmatrix} \begin{bmatrix} \Delta\phi \\ \Delta\theta \\ \Delta\psi \end{bmatrix} \quad (10)$$

which shows the coupling between control channels. The transient response curves in figure 9 also show the coupling. For example, roll is not coupled into either pitch or yaw. However, both pitch and yaw motion are coupled into the other two axes; that is, pitch motion is coupled into both roll and yaw, etc. Therefore, the simulation results agree with the behavior predicted by the analytic study.

The response of the system with each processor to a multiple axis error is shown in figure 10. The initial attitude errors are 5° about each control axis. The corresponding initial gimbal angles are $\beta_{10} = 34.1$, $\gamma_{10} = 30.3$, $\beta_{20} = 6.7$, and $\gamma_{20} = 46.4$. The commanded gimbal angles are the same as for the runs shown in figures 7, 8, and 9 (table 1). Runs (a), (b), and (c) in figure 10 show the response of the system using the ideal, partial, and constant processors, respectively. Although the system using the partial processor does exhibit slightly more overshoot, the response of the system is very similar with each processor.

The influence of nonzero initial system momentum on the behavior of the system was investigated on the simulator. The investigation was divided into two categories: (1) the effect of initial momentum stored about a control axis perpendicular to the axis of rotation and (2) the effect of initial momentum about the axis of rotation. The initial momentum of the system was stored in the motors only; that is, the initial table rates are zero. The momentum was stored in a single motor with a magnitude less than 60 percent of the maximum motor momentum. Since the effect of initial momentum on the behavior of the system depends mainly on the characteristics of the motor, only the ideal processor was used for all runs.

The influence of initial momentum about an axis perpendicular to the axis of rotation is negligible for reorientations of 5° or less. For example, runs were made with initial momentum in the roll motor equivalent to 60 percent of its maximum and a yaw attitude error of 5° . The difference between the runs with 60 percent initial momentum and zero initial momentum was negligible.



Sketch (d)

The effect of the initial momentum about the axis of rotation on the system response is significant; that is, the initial momentum and position error are about the same control axis. The characteristics of the motors result in the torque-speed curve given in sketch (c). Assume that the initial wheel speed of the yaw motor corresponds to point 1 in sketch (c). The initial attitude error is also about the yaw axis and corresponds to point 1 in sketch (d). As the attitude error is diminished, the wheel speed increases toward point 2 (sketch (c)). At point 2, the attitude error has diminished enough that the lead information causes the voltage to the motor to change sign. The motor is then operating at point 3. Therefore, a high torque is available for decelerating the satellite and the overshoot should be negligible. In contrast, assume the motor is initially operating at point 5. As the attitude error is reduced, the motor speed increases from point 5 to point 6. At point 6, the motor voltage again changes sign to decelerate the satellite. With the motor now operating at point 7, the torque available is small and the overshoot is significantly larger than in the previous case.

The effect of initial motor momentum about the axis of rotation on the behavior of the system is shown in figure 11. The initial attitude error is 5° about the yaw axis. The response of the system with zero initial wheel speed is shown in run (a). (The initial angular velocity of the table is zero. Also the frequency of the noise on the traces is so high that it does not affect the transient behavior.) Run (b) shows the response of the system for an initial yaw wheel speed of 60 percent of the maximum. The overshoot in run (a) is less than 10 percent while the overshoot in run (b) is approximately 80 percent. Consequently, the initial wheel speed does have a significant effect on the behavior of the system. It would therefore be advantageous to include the wheel speed information in calculating the control voltage to minimize the effect of initial wheel speed.

Steady-state behavior- The steady-state behavior of the system is a function of the momentum of the motors when the system is stabilized. If the motor is operating at a constant speed when the system is stabilized, a back emf voltage exists. In order for the motor to continue spinning at a constant speed, a control voltage equal and opposite to the back emf must exist. The

existence of the control voltage implies an error in the attitude of the satellite. This error is called the steady-state pointing error or offset error.

The steady-state pointing error (offset) for a specific loop gain is ideally proportional to the wheel speed. For the ideal processor, the theoretical offset error as a function of wheel speed is given as the solid lines in figure 12. The figure shows the offset error for various gains. For example, if the wheel speed is 600 rpm and the gain $K_c = 1000$, the offset error is 0.29°.

The results of the simulation show the same trends as the theoretical results (fig. 12); that is, the offset error increases as the wheel speed increases. However, a comparison of the magnitudes of the offsets shows poor correlation between the simulation and analytic results. The correlation between the results is better for the lower gains but becomes poorer as the gain increases. For the higher gains, the offset error does not appear to be a function of gain; that is, an increase in K_c from 4700 to 9400 does not result in an equivalent reduction in the offset error. In fact, the offset error is small but random.

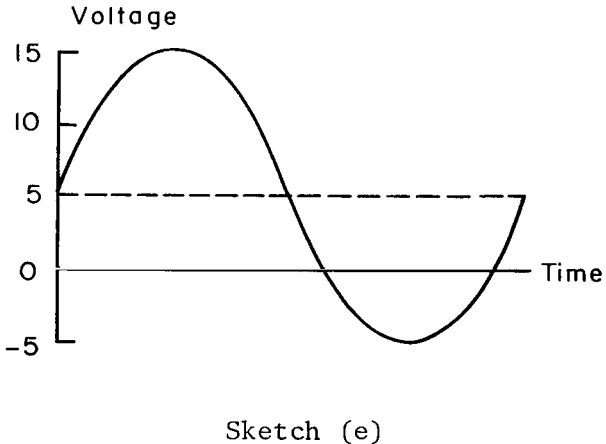
The poor correlation between the simulator and the theoretical results is caused by the sensitivity limit of the sensors and noisy control voltages. For the higher gain cases, the offset errors are random because the offset magnitude and the sensor sensitivity magnitude are about equal. Thus, one is trying to point the vehicle to an accuracy equal to or better than the available attitude information.

Noisy control voltages also cause a poor correlation between the simulator and the theoretical results. The source of the noise is not important but

is not generated by the processor. To show the correlation between offset error and noise, consider as an example the system at equilibrium with an offset error of 6 minutes of arc. Assume this offset error is equivalent to a 5 V d.c. signal to the motor which cancels the back emf voltage. Assume that the voltage to the motor has a noise component of $10 \sin \omega t$ superimposed on the d.c. signal (sketch (e)). If the voltage to the motor is limited to ± 15 V, the average voltage to the motor is +5 V. If the voltage to the motor is limited to ± 10 V, the average signal to the motor is less than 5 V. Since the

d.c. motor responds to the average signal, the motor requires +5 V average for the system to be at equilibrium. Therefore, the pointing error must increase until an average of +5 V is being transmitted to the motor.

The noise on the control voltage does not influence the pointing accuracy of the system if its magnitude is not limited. However, if the noisy signal



Sketch (e)

is limited, the pointing accuracy becomes poorer. The effect of the noise can be reduced by introducing a high frequency filter prior to the lead network. The break frequencies chosen for the lag network were found to eliminate some of the high frequency noise but not influence system stability.

Large Angle Results

Both the analytic study and the simulation results indicate the behavior of the system with the partial processor is quite adequate for small angles. The large angle maneuvers were made for a few of the many possible initial conditions. The conditions were, in general, randomly chosen but in some instances were chosen so that the system would operate in the more severe regions. The simulation runs should provide an indication of how well the partial processor will control the satellite through larger angles.

Large angle slew- A number of large angle reorientations were made on the simulator to show the behavior of the system using the partial processor. The results of one reorientation are shown in figure 13. The initial system momentum is zero; that is, the initial wheel speeds as well as initial table rates are zero. The initial and commanded gimbal angles are given in table 2 with their corresponding Euler angles. The gains and compensator time constants are also given in the table.

TABLE 2.- DATA FOR FIGURE 13

	β_1	γ_1	β_2	γ_2	ϕ	θ	ψ
Initial	30.8	18.9	9.5	36.4	-5.0	+5.0	+72.0
Command	-19.8	28.2	31.0	28.4	+5.0	-5.0	+20.0

$$K_c = -4700 ; \quad d_{12} = 1.0 ; \quad T_1 = 4.55 ; \quad T_2 = 0.455 ; \quad T_L = 0.22$$

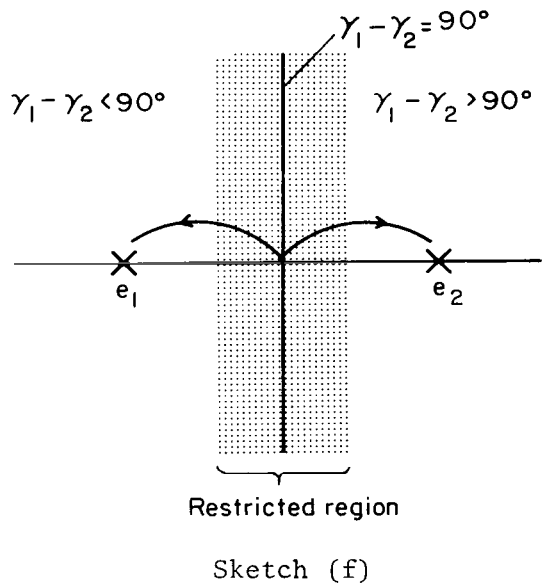
A comparison of the initial and final Euler angles indicates that the major component of the maneuver is about the yaw axis. It is observed from figure 13 that the linear estimate of the error ($\Delta\phi$, $\Delta\theta$, $\Delta\psi$) is driven from its initial value to zero. The system does overshoot but is well behaved.

The pointing accuracy of the system, as previously indicated, is influenced by noisy control voltages if the signals are limited. The motor voltage saturation level was reduced for the large angle reorientations to insure the table rate would not exceed the tracking rate of the star trackers. Since the limiting is now more severe, the noise on the motor voltages has a more dramatic effect. Consequently, the pointing error for the run was 0.18° . (The pointing error in this instance is the vector sum of the individual errors about each control axis.) This pointing error could have been reduced by increasing the saturation limits as the system approached the equilibrium point.

System behavior near the restricted region- The actual path of rotation is more difficult to predict for large angle reorientations. It is therefore more difficult to insure that the response trajectory will not enter the restricted region. One might ask the following questions: "Could the partial

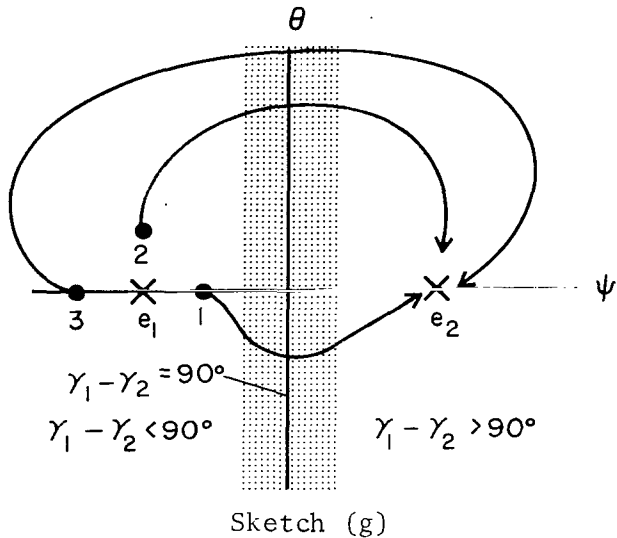
processor be used to control the system in and through the restricted region? How is the behavior of the system affected if the region of restricted operation is penetrated during transition from the initial to the commanded position (see sketch (b) - trajectory a)? Does the system respond satisfactorily when the initial and commanded positions are on opposite sides of the restricted region (sketch (b) - trajectory b)?" The following conditions were investigated: (1) the initial and commanded positions on the same side of the restricted region; (2) the initial position within the restricted region; (3) the initial and commanded positions on opposite sides of the restricted region.

The system behaves satisfactorily when the initial conditions are outside the restricted region (same side as command) regardless of whether or not the response trajectory entered the restricted region. However, at the indeterminant condition, attitude information about an axis perpendicular to the plane formed by the lines of sight to the two stars is not available from the gimbal angle measurements. Thus, the system does not respond to an error about this axis. An extrapolation of this result implies that the component of system response parallel to the plane of indeterminancy is the most critical maneuver near the restricted region. This component of response becomes less critical as the system operation occurs further away from the indeterminant condition. Just how far from the indeterminant condition the system must operate to behave satisfactorily depends on the quality of the star trackers. With good quality star trackers, the present restricted region ($80^\circ < |\gamma_{1c} - \gamma_{2c}| < 100^\circ$) might be large enough. However, if the tracker quality is poor, the magnitude of the region may have to be increased.



The system also responded satisfactorily when the initial position was inside the restricted region. The commanded gimbal angles were chosen so that the equilibrium points are 13° away from the indeterminant condition; that is, $|\gamma_{1c} - \gamma_2| = 77^\circ$ or 103° . The initial conditions were chosen so that the system started at the indeterminant condition. When $d_{12} > 0$, the system stabilized at e_1 (sketch (f)). When $d_{12} < 0$, the system stabilized at e_2 in the region $(\gamma_1 - \gamma_2) > 90^\circ$. Since the initial and commanded angles were the same for the above two runs, the examples clearly show the multiple equilibrium points, and the satisfactory response when operation begins in the indeterminant region.

The behavior of the system in traversing the restricted region was also investigated. Here the command angles were chosen so that the two equilibrium points (e_1, e_2) are about 17° from the indeterminant condition. The points 1,



2, and 3 represent possible initial conditions (sketch (g)). The commanded gimbal angles are $\beta_{1c} = -0.1^\circ$, $\gamma_{1c} = 90.8^\circ$, and $\beta_{2c} = 39.0^\circ$. If $d_{12} > 0$, the command corresponds to a stable equilibrium point e_2 at ($\phi = 0$, $\theta = 0$, $\psi = 40.3^\circ$) and an unstable equilibrium point e_1 at ($\phi = 0$, $\theta = 0$, $\psi = 73.3^\circ$). The indeterminant condition occurs at ($\phi = 0$, $\theta = 0$, $\psi = 57^\circ$). The initial wheel speeds as well as table angular rates are zero. The behavior of the system whose initial condition corresponds to point 1 and commanded position corresponds to e_2 is shown in figure 14. Although the system is driving toward the desired equilibrium

point, one observes that the voltage from the partial processor in the yaw direction (ϵ_ψ) increases until the system passes through the indeterminant condition. The voltage then decreases to zero. Since the voltage must go to zero at each equilibrium point, an extremum between the points is expected. The occurrence of the indeterminant condition can be determined by observing the gimbal angle response traces (β_1 , γ_1 , β_2 , γ_2) and noting when $|\gamma_1 - \gamma_2| = 90^\circ$.

The trace of the Euler angle (θ) indicates that the system pitches to -6° and then returns to zero as the system approaches the equilibrium point. This behavior occurs because the pitch axis is almost parallel to the axis perpendicular to the indeterminant plane during the maneuver. Therefore, very little attitude information exists about the pitch axis and the observed motion is expected. Also, the momentum increase in the roll motor (WR1) indicates the existence of an undesirable torque. (The response of the system with initial position at point 2 is also shown in sketch (g).)

The behavior of the system starting at 3 (sketch (g)) and commanded to drive to e_2 could not be simulated on the air bearing table because the table motion is so large that the trackers translate out of the 12-inch star bundle. Therefore, the condition was simulated on the digital computer. The initial attitude of the table is $\phi = 0^\circ$, $\theta = 0^\circ$, $\psi = 80^\circ$. Also, the initial wheel speeds and table rates are zero. The results show that the table, as expected, initially drives away from the unstable equilibrium point e_1 (sketch (g)). The system then begins to maneuver around e_1 , passes through the restricted region, and stabilizes at e_2 . The pitch and yaw Euler angles are measured along the rectangular coordinate system in the sketch. Although the system did drive to the desired position, the response trajectory is undesirable. Operationally, a more desirable maneuver would be to command the system to first drive to point 1 and then command e_2 .

CONCLUSIONS

Three methods of processing the star tracker gimbal angle measurements to derive attitude control signals for a satellite were simulated with actual spacecraft type hardware. The three methods are called the ideal, partial, and constant processors. The ideal processor is the mechanization of the first-order approximation of the exact nonlinear equations. The partial and constant processors are simplifications of the ideal. The results of the simulation for small-angle commands are as follows: (1) The system using each processor performed as predicted by the prior theoretical study. (2) Initial momentum about the axis of rotation could adversely affect the transient behavior. It would be advantageous therefore to include the inertia-wheel speed information in the calculation of the attitude control signals. (3) Noise in the control loop (not generated by the processors) could adversely affect the steady-state pointing error. If the magnitude of the noise is limited by the saturation type nonlinearity and direct current motors are used, the pointing error increases. (4) An error in measuring the gimbal angles could cause a considerable shift in the equilibrium position. Under normal conditions, the magnitude of the error in gimbal measurement and the magnitude of the shift in equilibrium position are approximately equal. However, if the system is operating near the indeterminant condition, the shift in the equilibrium position could be five to ten times as large as the error in the measurement.

The large angle results showed the following: (1) The system using the partial processor stabilized the air-bearing table for reorientations as large as 55°. (2) Although the table cannot be stabilized in the restricted region, the system with the partial processor might be used to maneuver the table through the region.

Ames Research Center
National Aeronautics and Space Administration
Moffett Field, Calif., 94035, March 11, 1970

APPENDIX

SIMULATION EQUIPMENT

The attitude control system was simulated by means of a Satellite Attitude Control Simulator (SACS) and a digital and analog computer. The SACS (fig. 2) includes an air bearing table that simulates the satellite. Two gimbaled star trackers which provide attitude information and three reaction wheels which provide the control torque are mounted on the table (fig. 3). The digital and analog computers are used to mechanize the processors and the passive lead networks (fig. 1). The digital and analog computers are not required to mechanize the control scheme but are used as a matter of convenience.

The air bearing table is shown in figure 2. The table has $\pm 29^\circ$ of motion in both pitch and roll and unlimited motion in yaw. With the equipment used for the simulation, the roll, pitch, and yaw inertias of the table were 196, 196, and 244 newton-meters² (145, 145, and 180 slug-ft²), respectively. The two star trackers and the yaw-motor-inertia wheel are mounted on the table as shown in figure 3. The pitch- and roll-motor-inertia wheel combinations are similarly mounted but are concealed in the figure.

The two star trackers are mounted on the table with their outer gimbal axes parallel to the roll axis of the table (fig. 3). As indicated in reference 1, this arrangement is required to provide the simplest processor to mechanize. The null position of tracker number 1 occurs when its optical axis is parallel to the table top and perpendicular to the outer gimbal axis. The null position of tracker number 2 occurs when the optical axis is perpendicular to the table top. Both gimbal axes of tracker 2 and the inner gimbal of tracker 1 are free to move through $\pm 50^\circ$. The outer gimbal axis of tracker 1 is free to move through more than $\pm 90^\circ$. Each tracker can track the star for rates to a maximum of $0.75^\circ/\text{sec}$. The gimbal angle readout device is a resolver with an accuracy of ± 10 minutes of arc.

The star trackers point at simulated stars that are mounted in brackets inside the vacuum chamber (fig. 2). The simulated stars have a clear aperture of 12 inches and provide a light source collimated to within ± 5 seconds of arc relative to the optical axis. The apparent star magnitude can be adjusted from -2 to +6.5.

Three mutually orthogonal motor-inertia-wheel combinations control the attitude of the table. The direct current motors have a time constant of approximately 35 seconds and a maximum angular velocity of 310 radians per second. The inertia of the motor-armature-inertia wheel combination is 0.019 newton-meters² (0.014 slug-ft²). The motor angular velocity can be determined from tachometer output signals.

Analog signals from the table such as star tracker gimbal angles, motor angular rates, and table angular rates are transmitted from the air bearing table to the digital computer where they are converted to digital form. The

measured gimbal angles are compared with the commanded gimbal angles to form gimbal angle errors. The gimbal errors are passed through the processors to obtain an estimate of the error as measured about the control axes. The calculation rate for the estimated errors (30 times a second) has a negligible influence on the control system behavior. The signals are converted from digital to analog form, passed through a lead network on an analog computer, and limited before being returned to the motors on the table.

REFERENCE

1. Showman, Robert D.; Doolin, Brian F.; and Sullivan, G. Michael: Simple Processors of Star Tracker Commands for Stabilizing an Inertially Oriented Satellite. NASA TN D-4490, 1968.

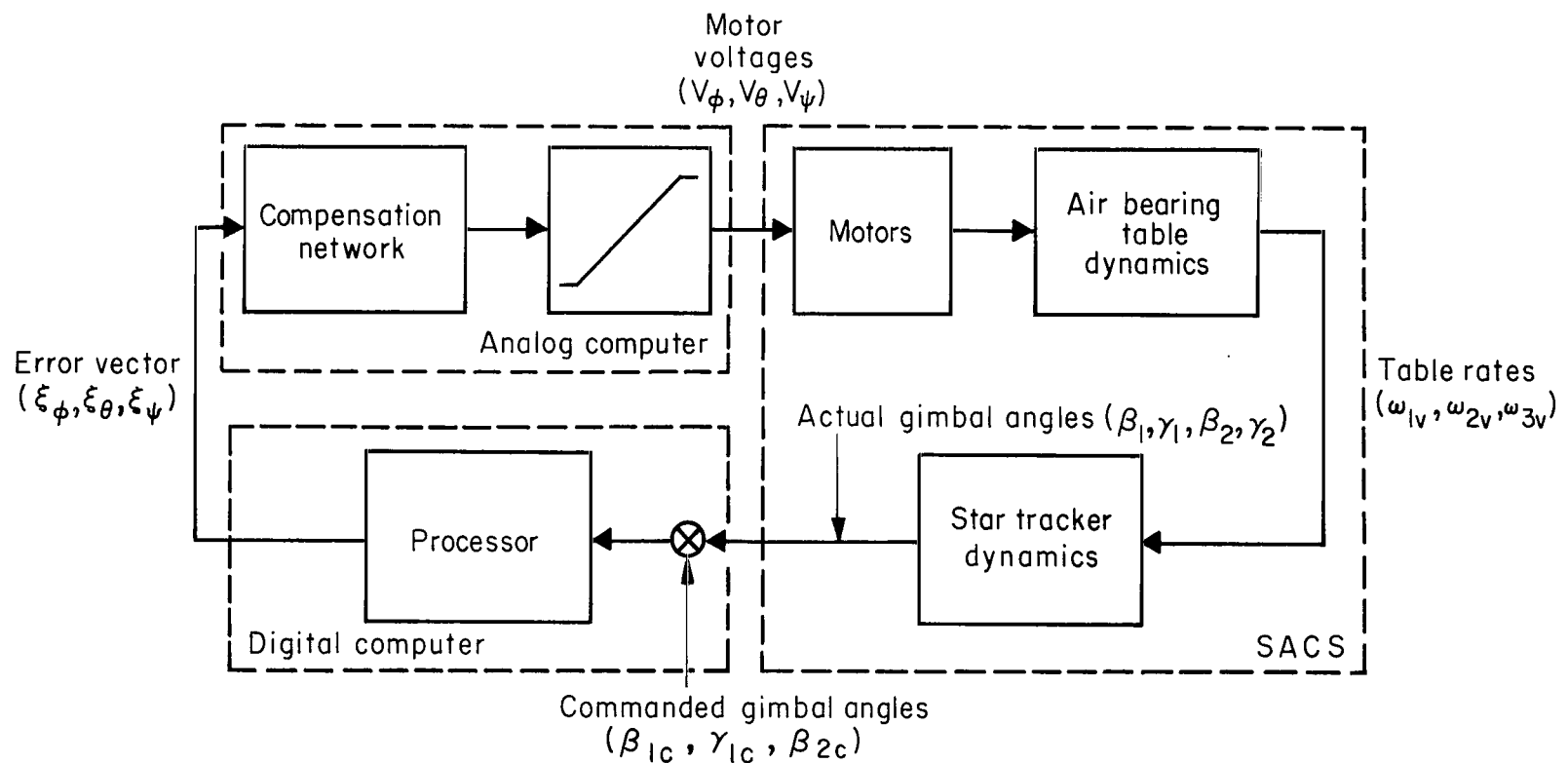


Figure 1.- Attitude control system.

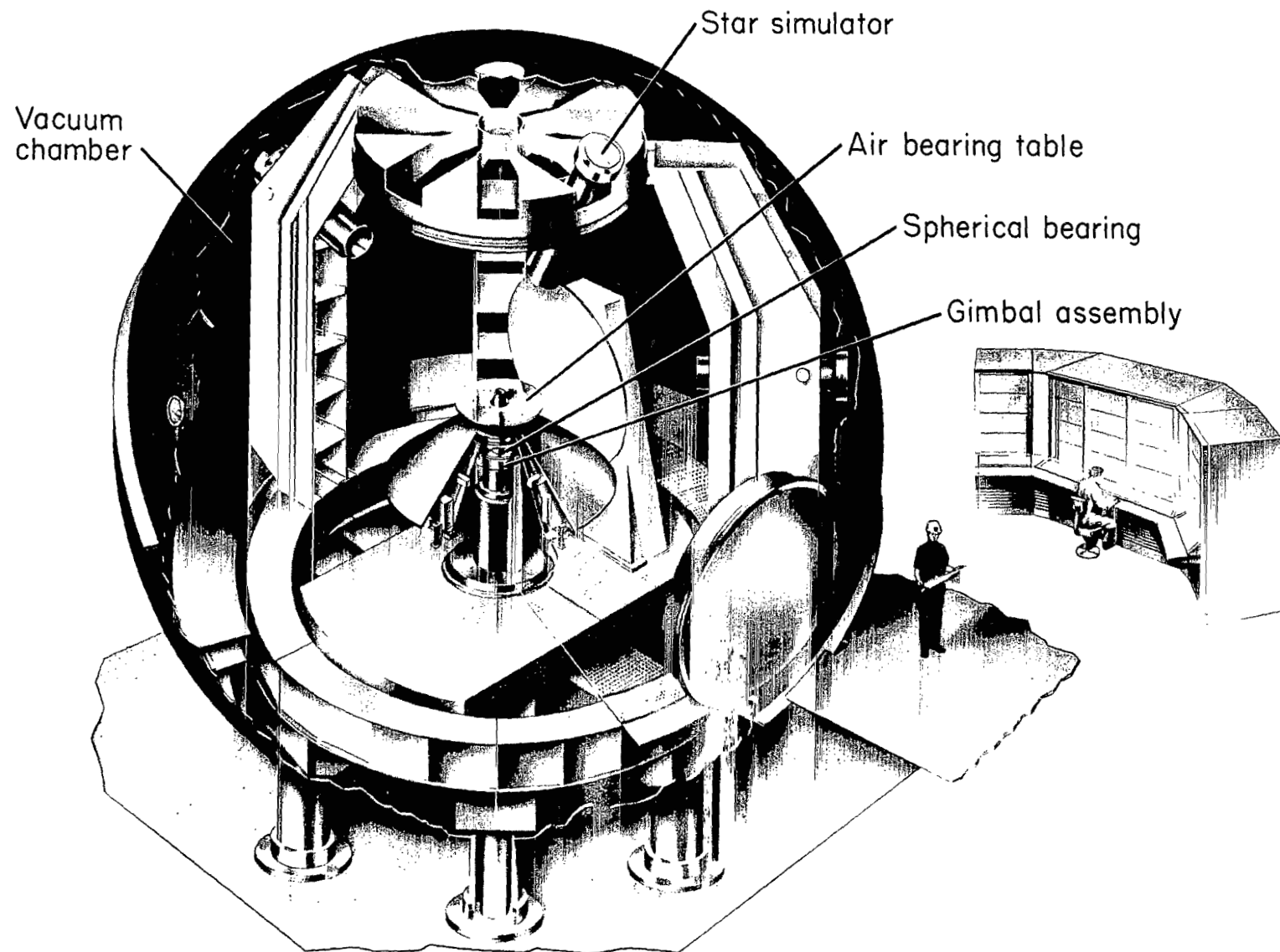


Figure 2.- Satellite attitude control simulator.

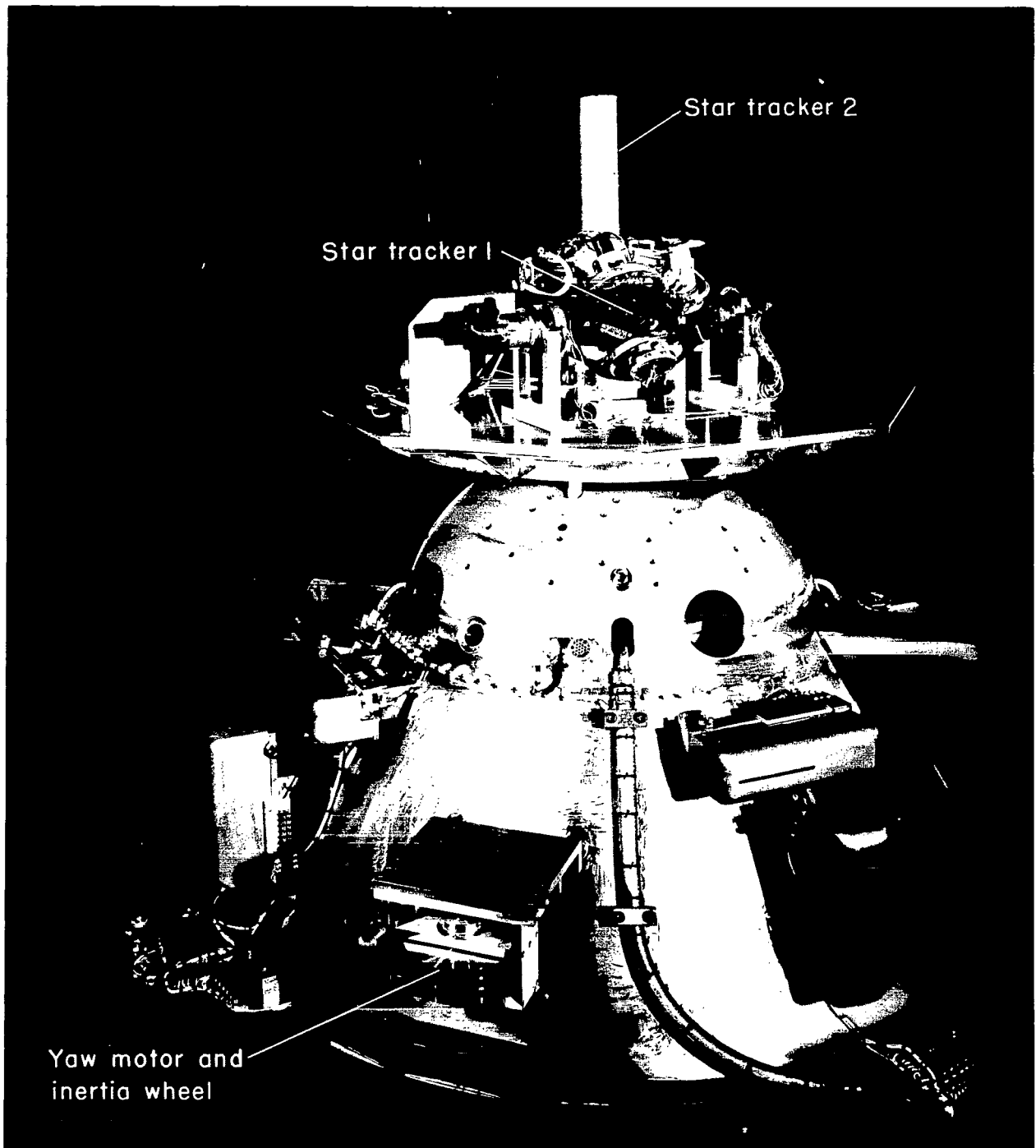


Figure 3.- Air-bearing table with equipment.

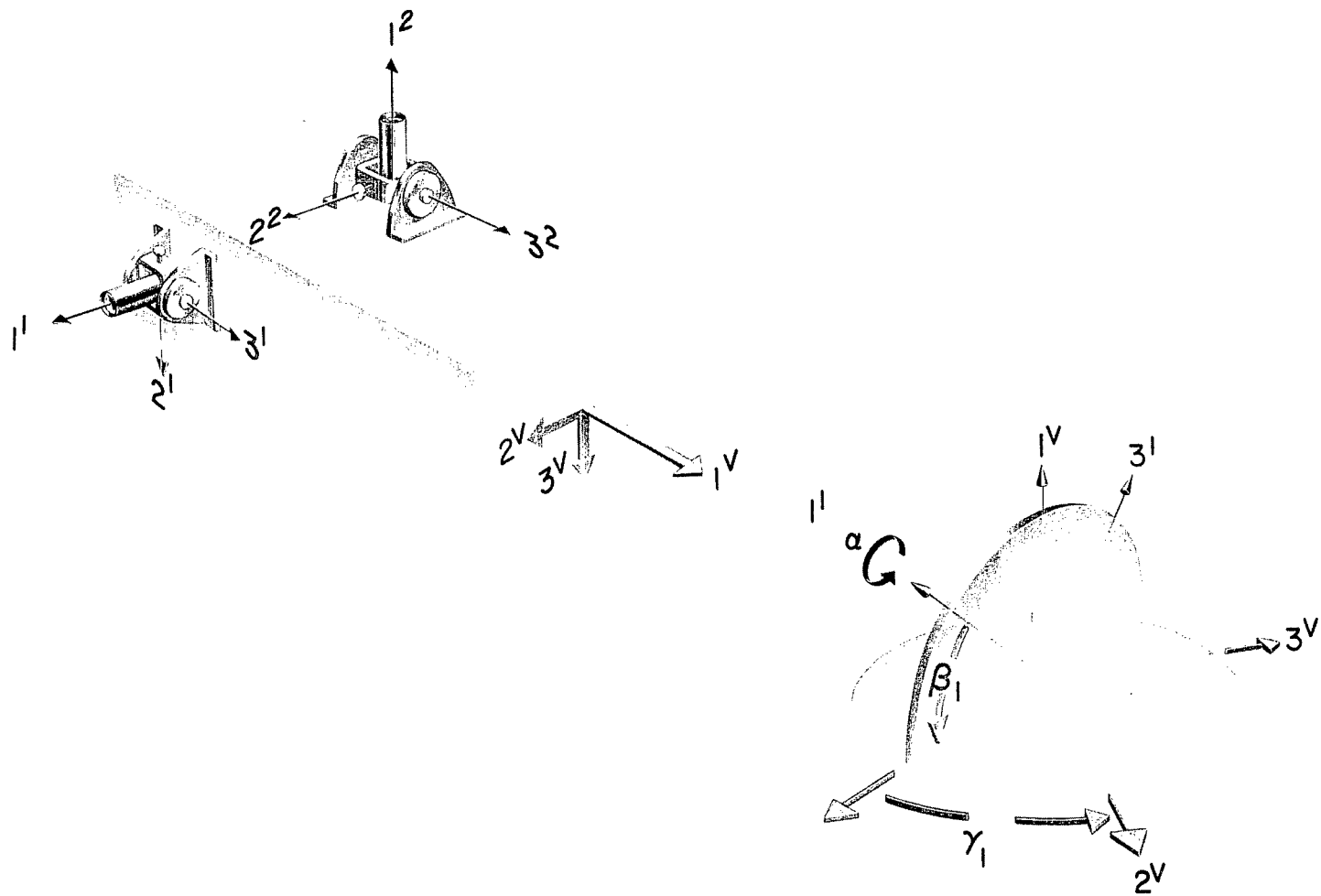
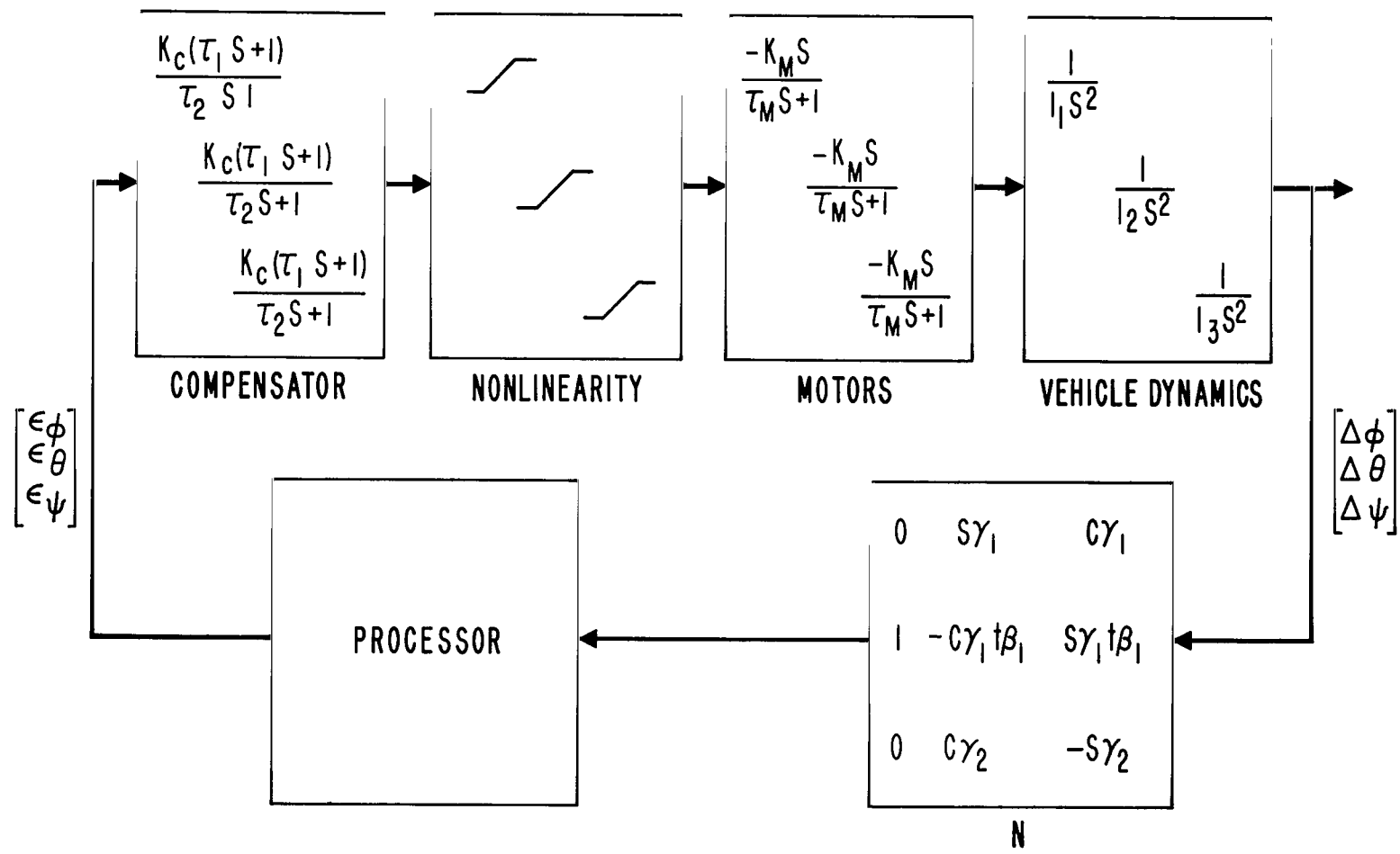


Figure 4.- Star tracker arrangement and gimbal angle illustration.



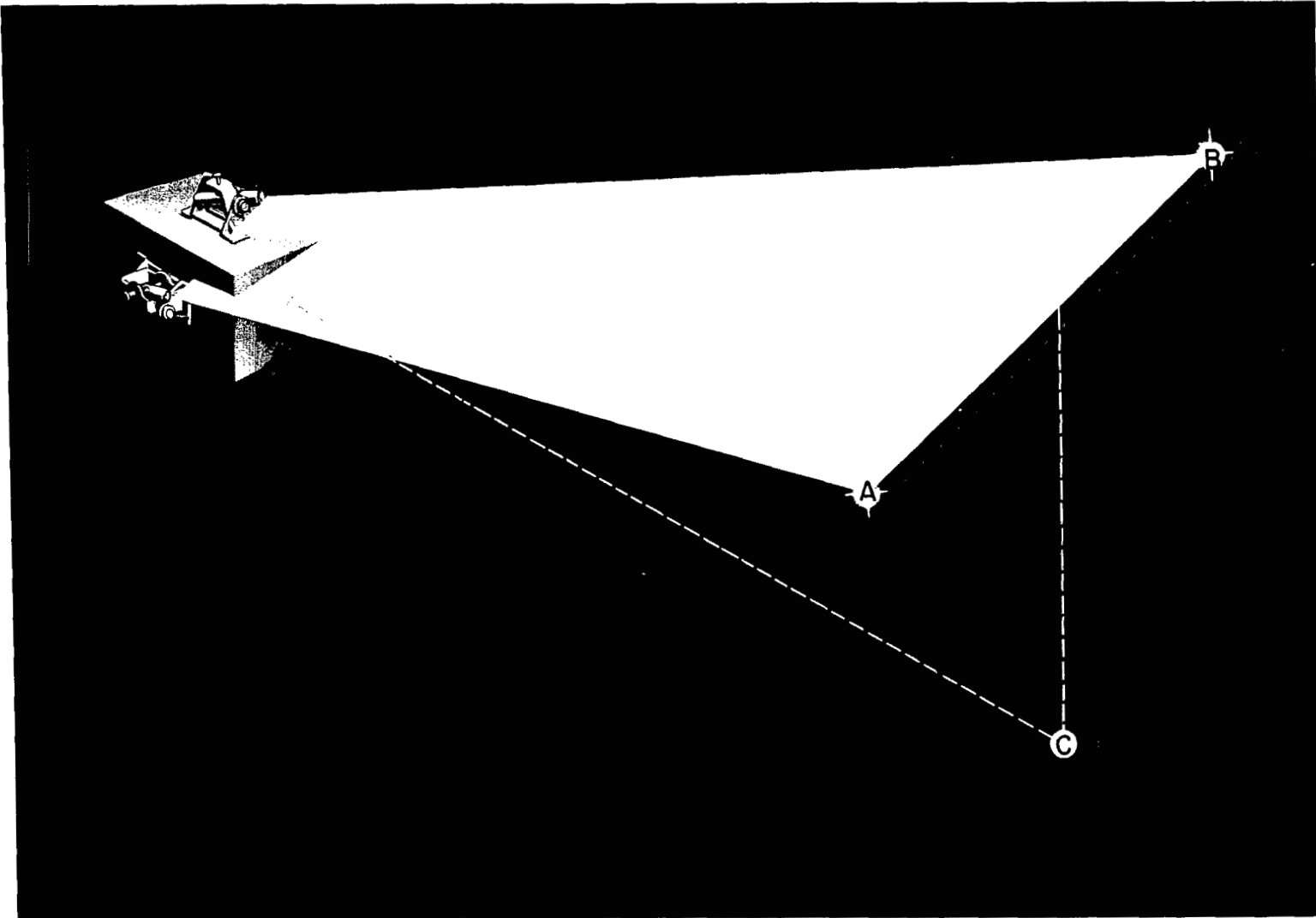
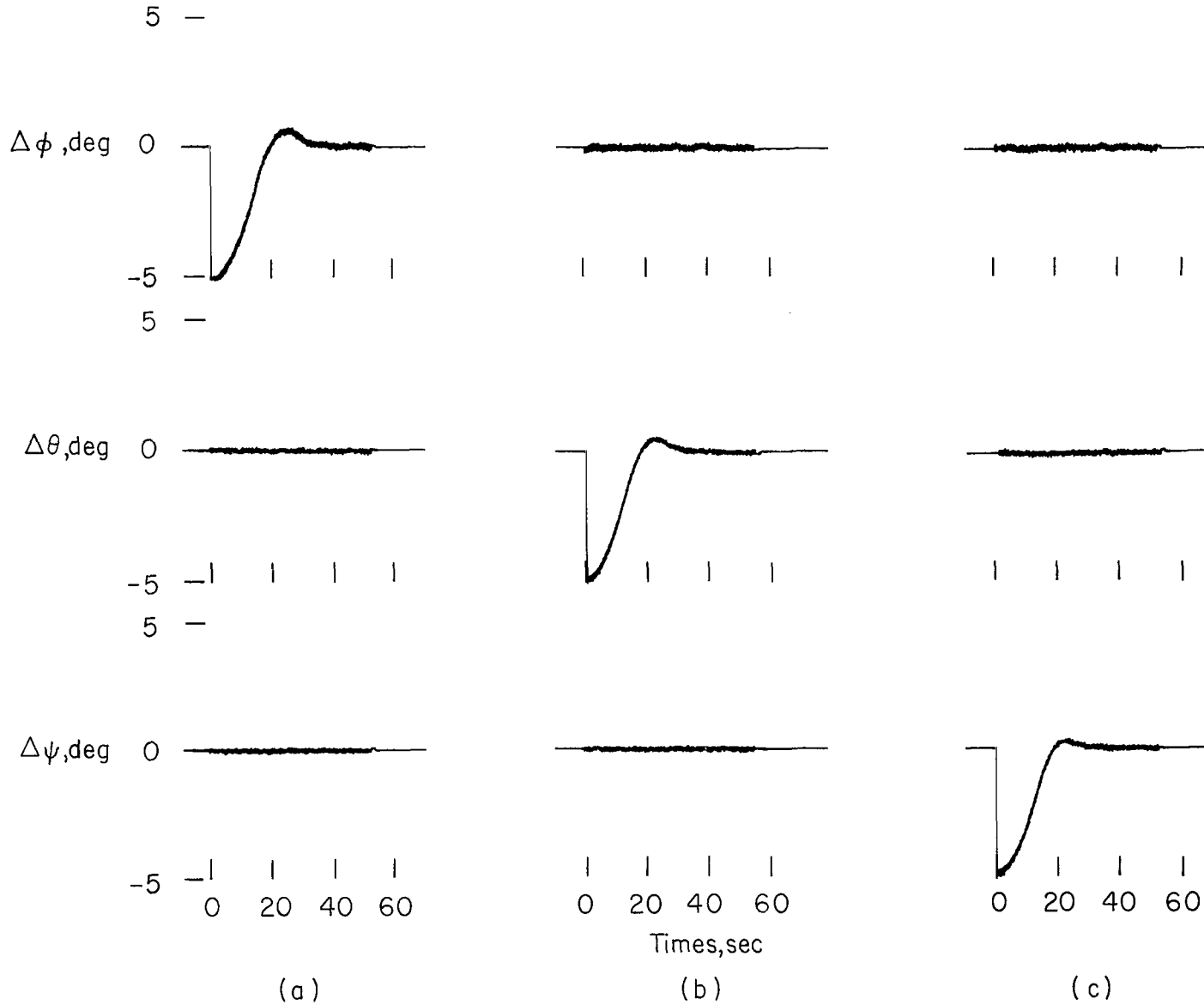


Figure 6.- Illustration showing when indeterminant condition would occur.



27

Figure 7.- Transient response of system using ideal processor with zero initial momentum.

5 —

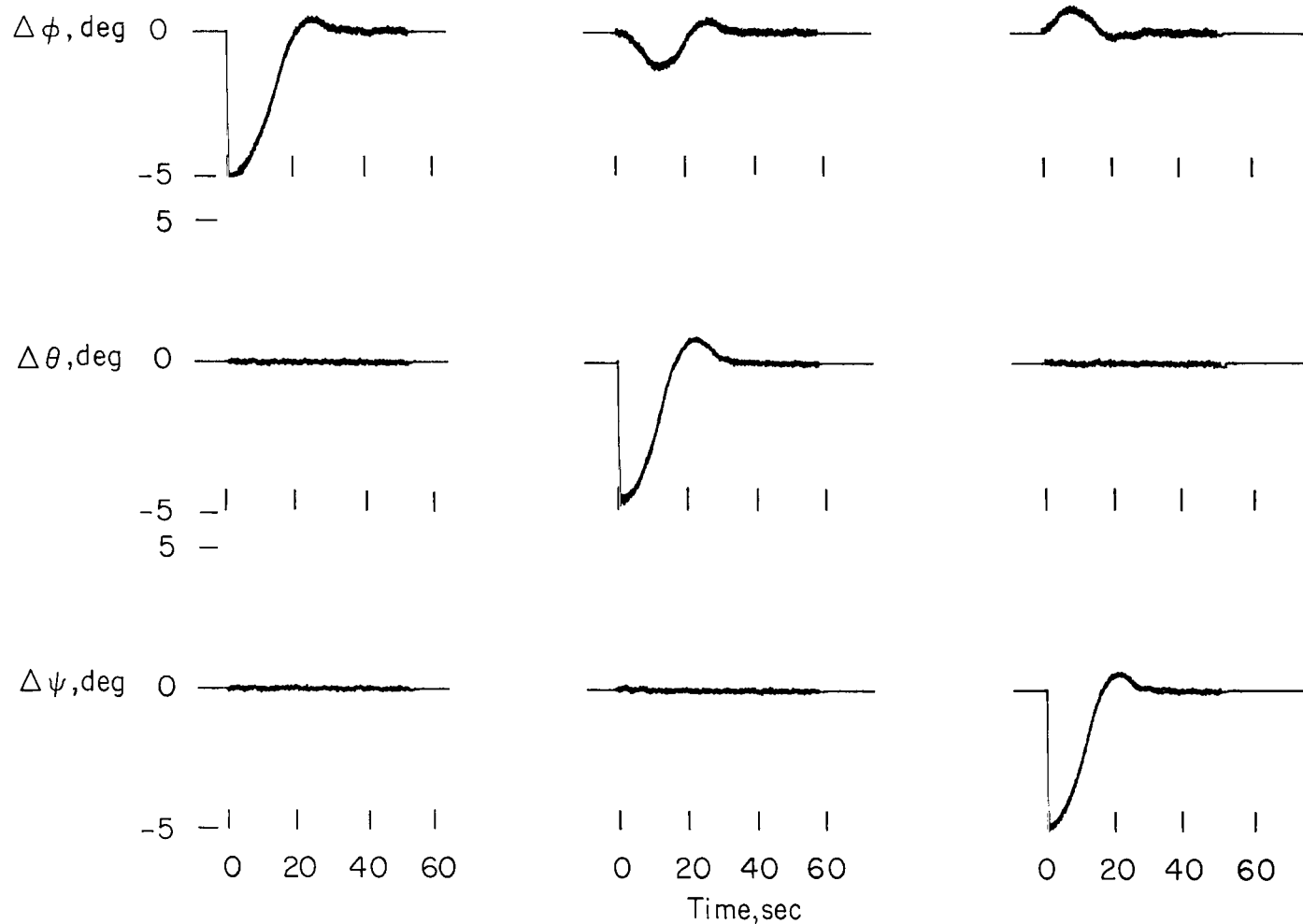


Figure 8.- Transient response of system using partial processor with zero initial momentum.

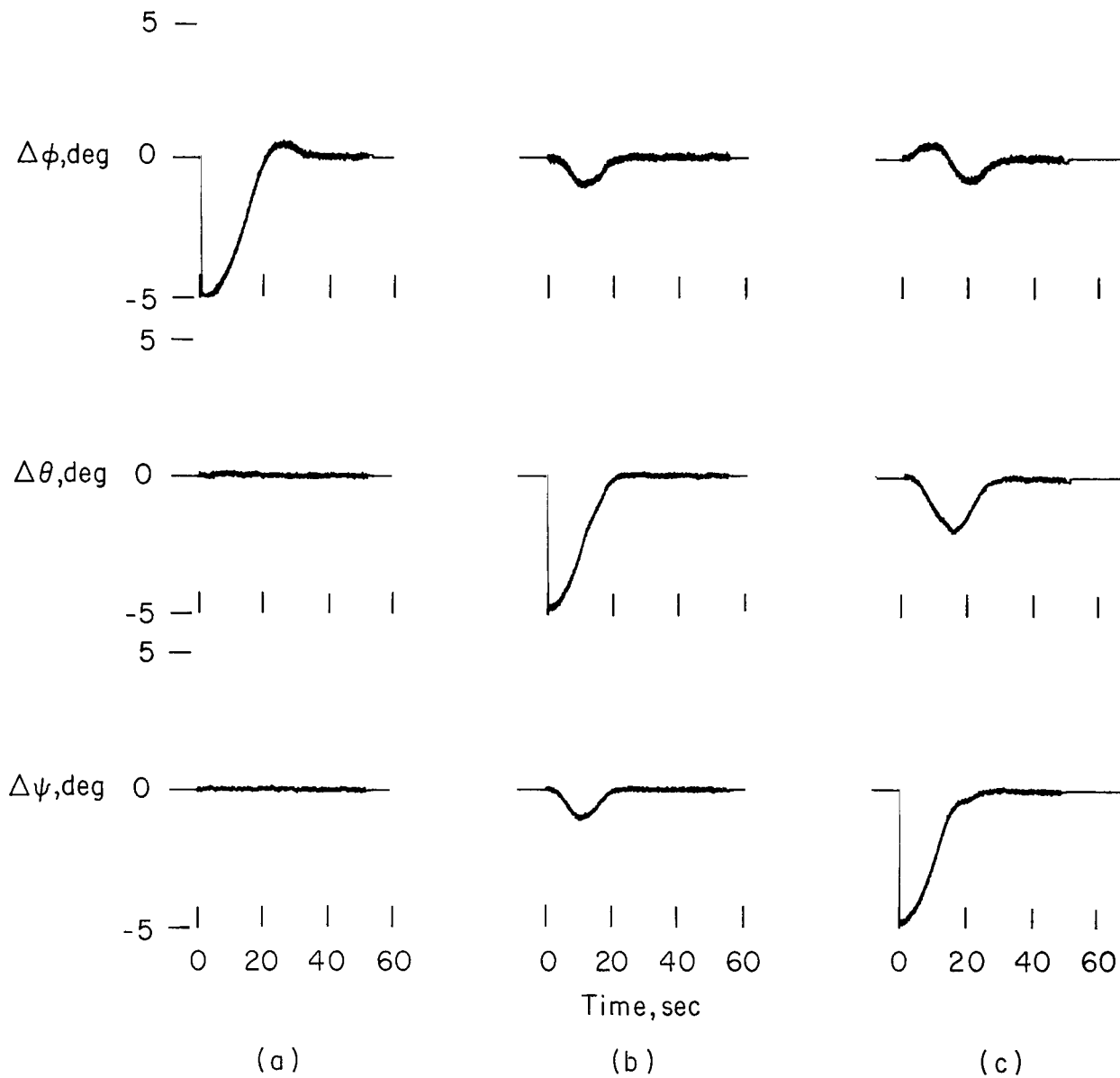


Figure 9.- Transient response of system using constant processor with zero initial momentum.

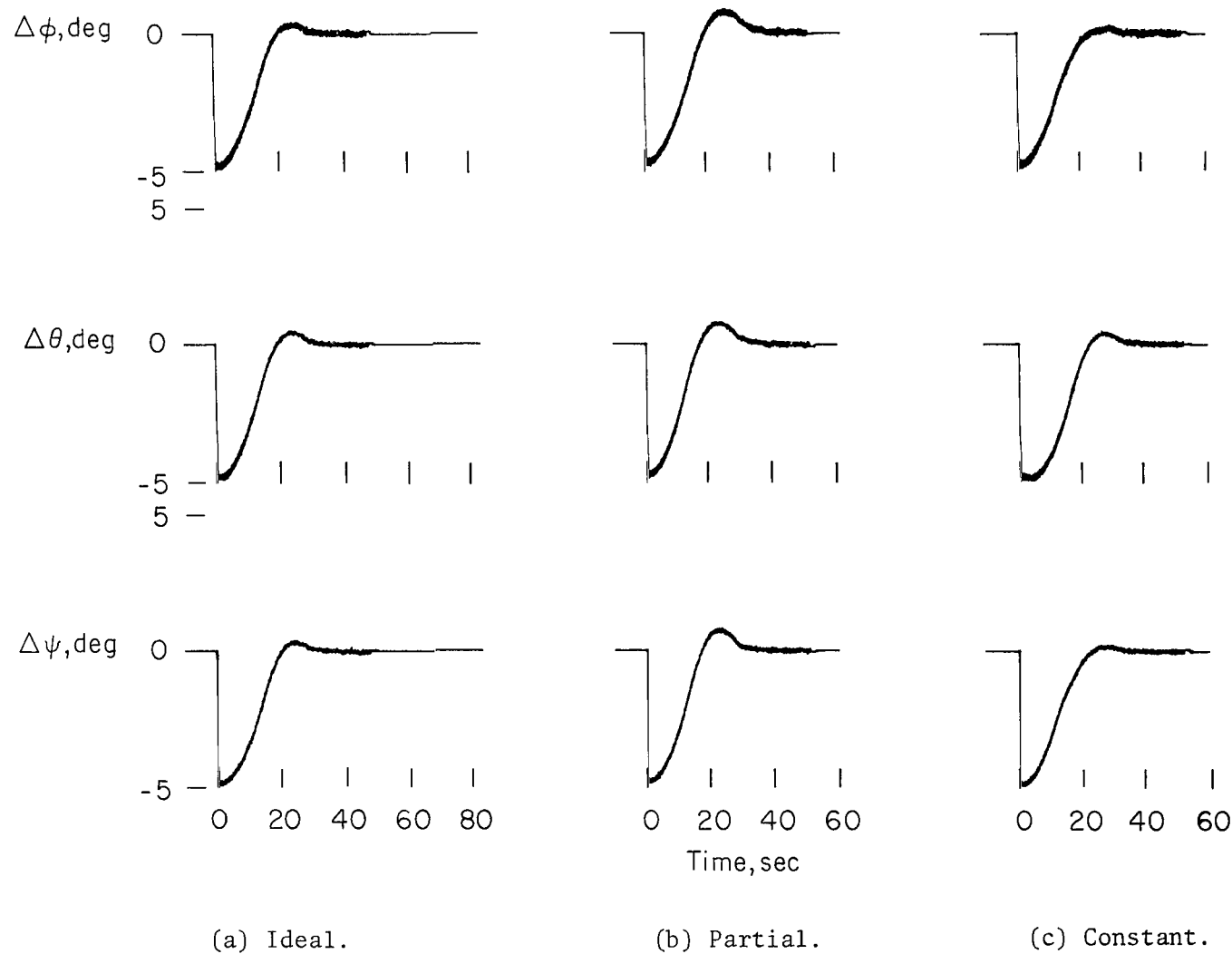
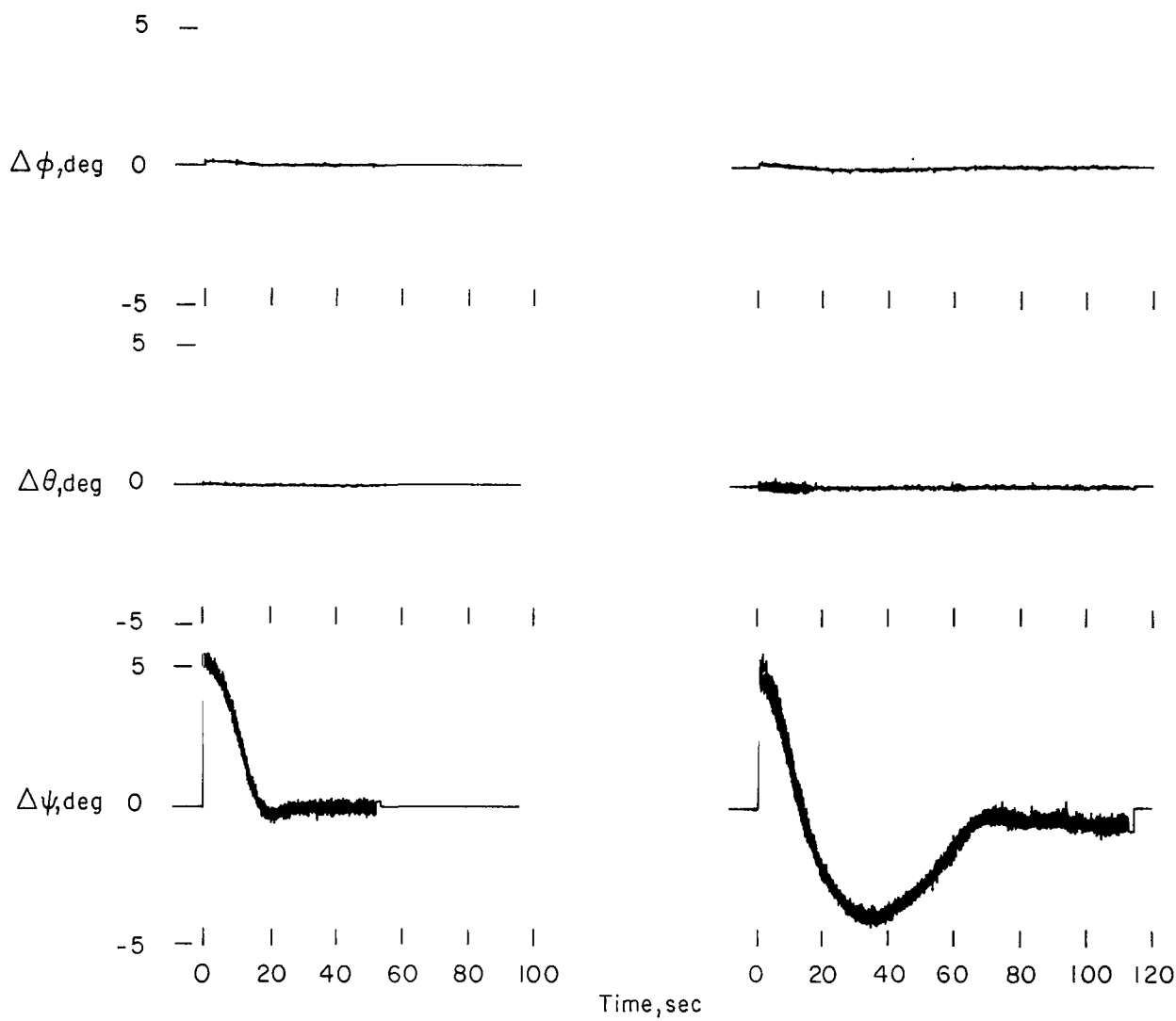


Figure 10.- Behavior of system using each processor to multiaxis error with zero initial momentum.



(a) System momentum = 0.

(b) System momentum = 60 percent
of maximum motor momentum.

Figure 11.- Effect of initial momentum on system behavior using the ideal processor.

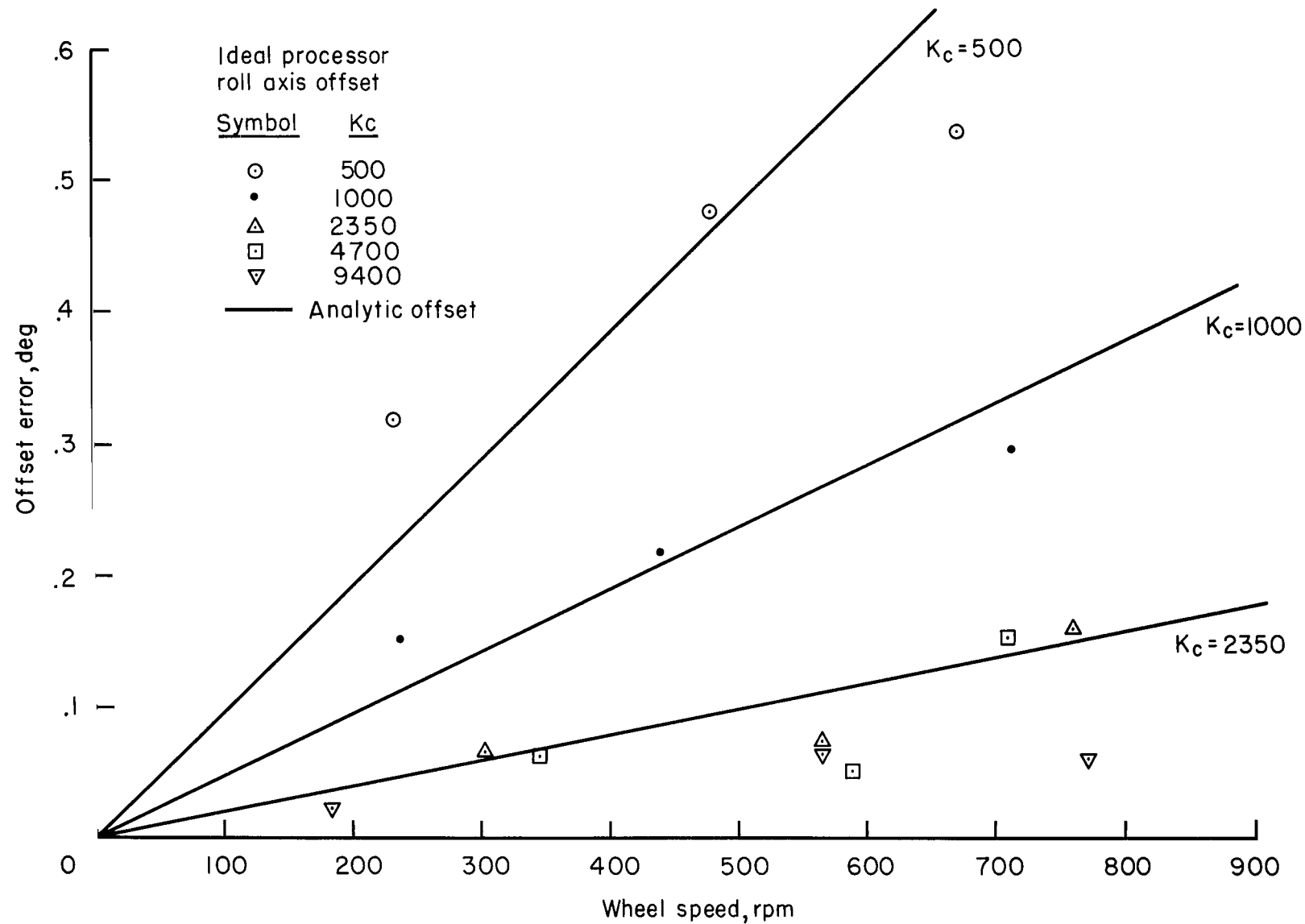


Figure 12.- Pointing error for system using ideal processor.

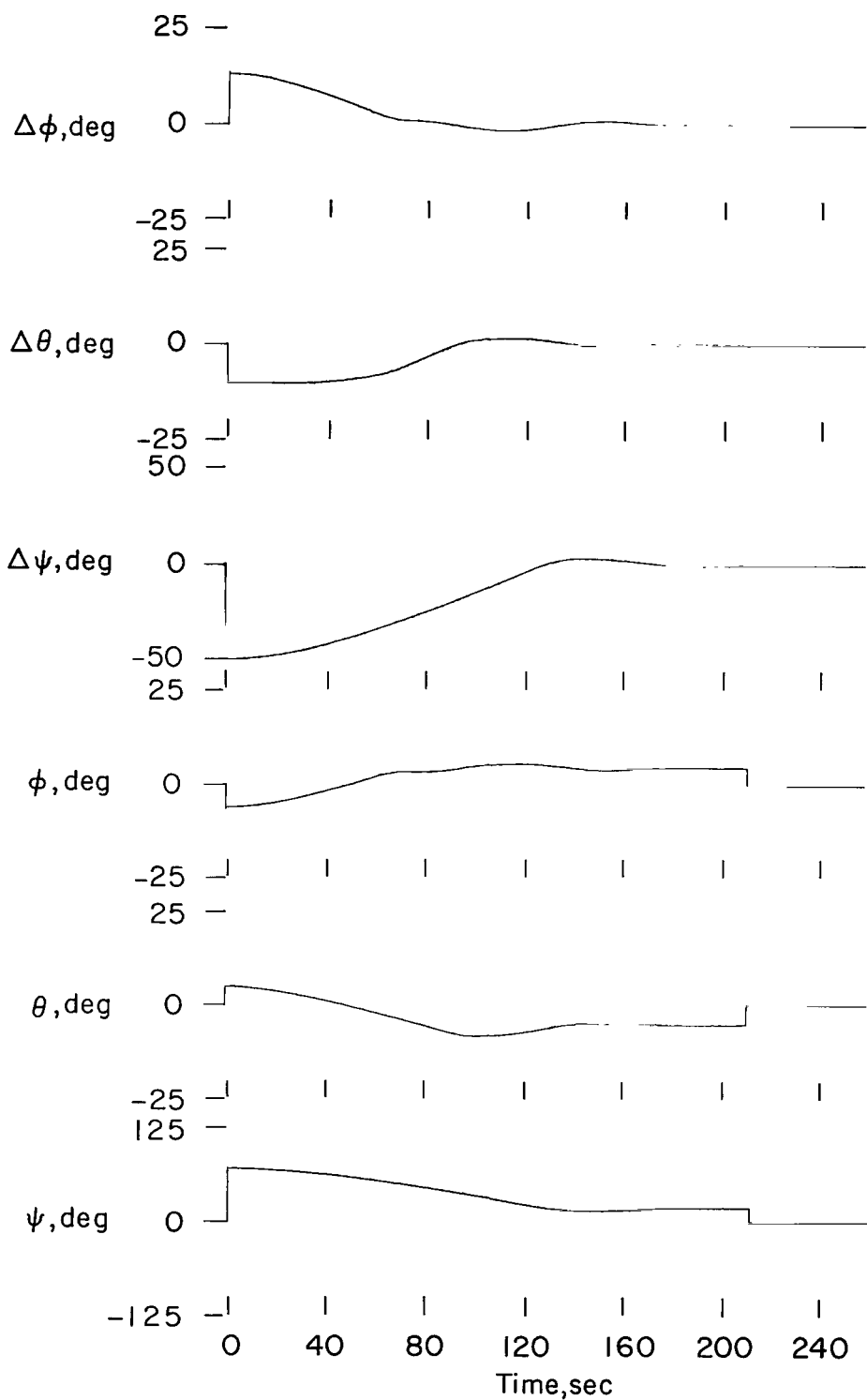


Figure 13.- Large angle reorientation using partial processor with zero initial momentum.

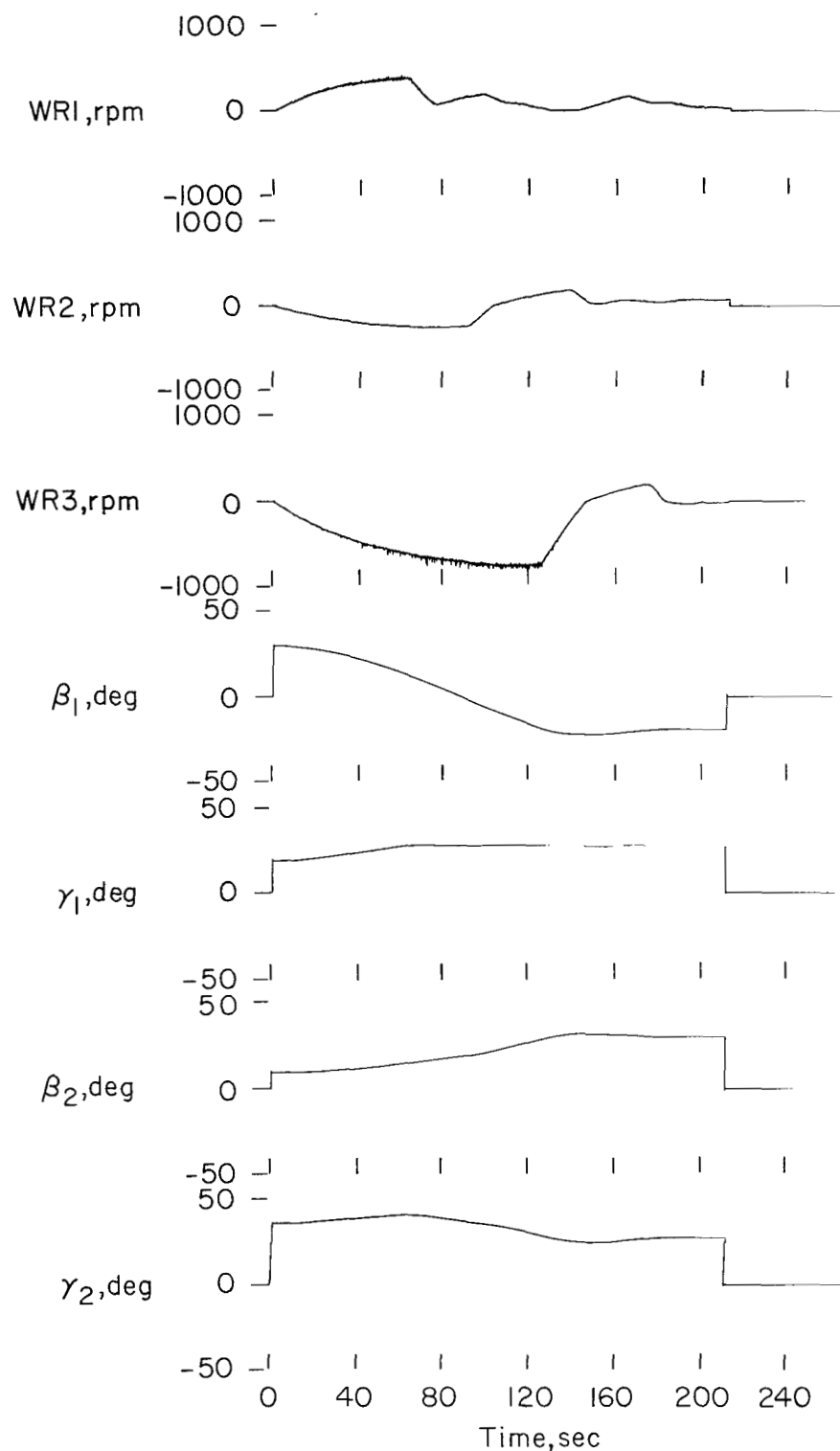


Figure 13.- Large angle reorientation using partial processor with zero initial momentum - Concluded.

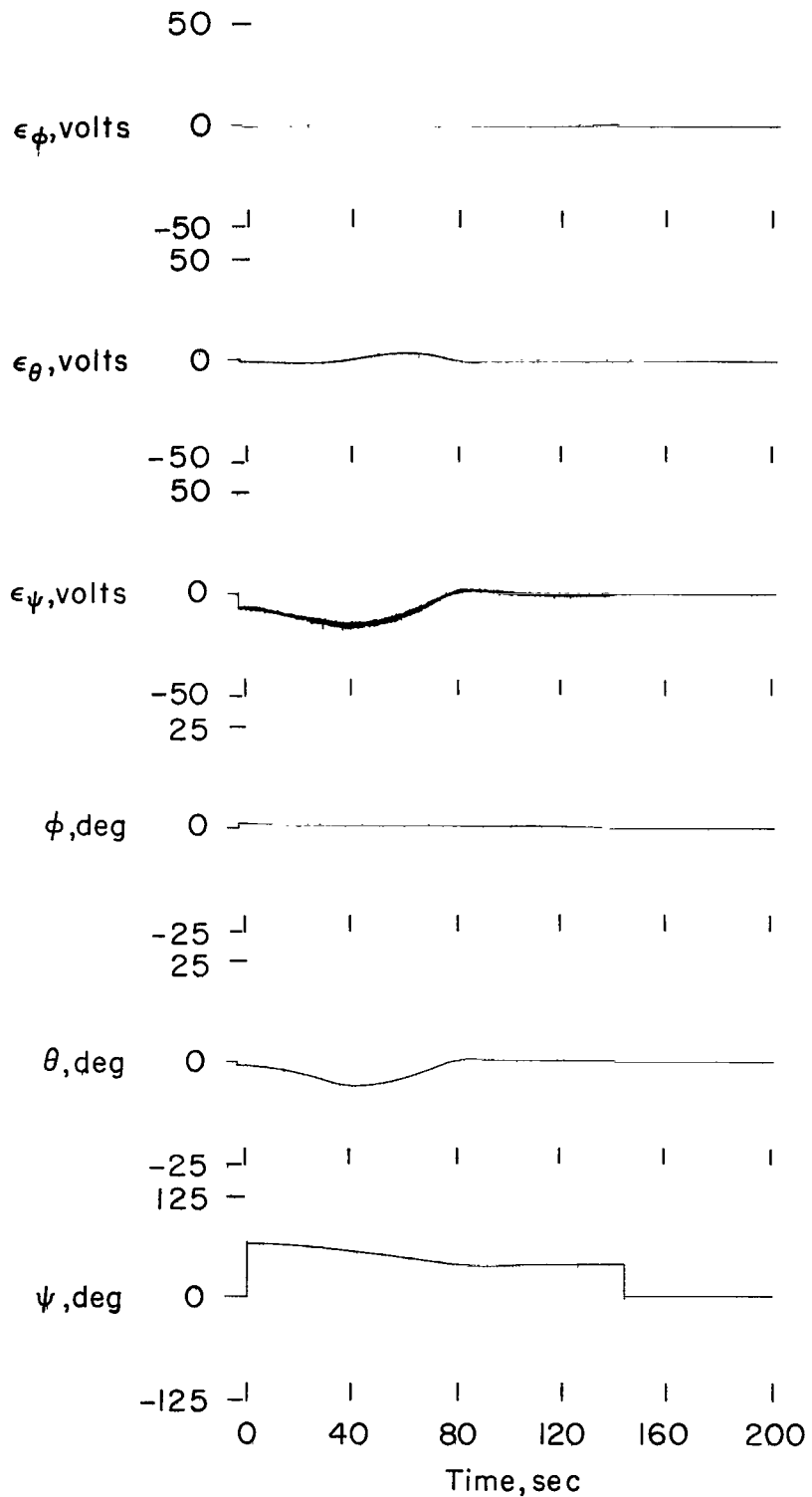


Figure 14.- Reorientation through restricted region using partial processor with zero initial momentum.

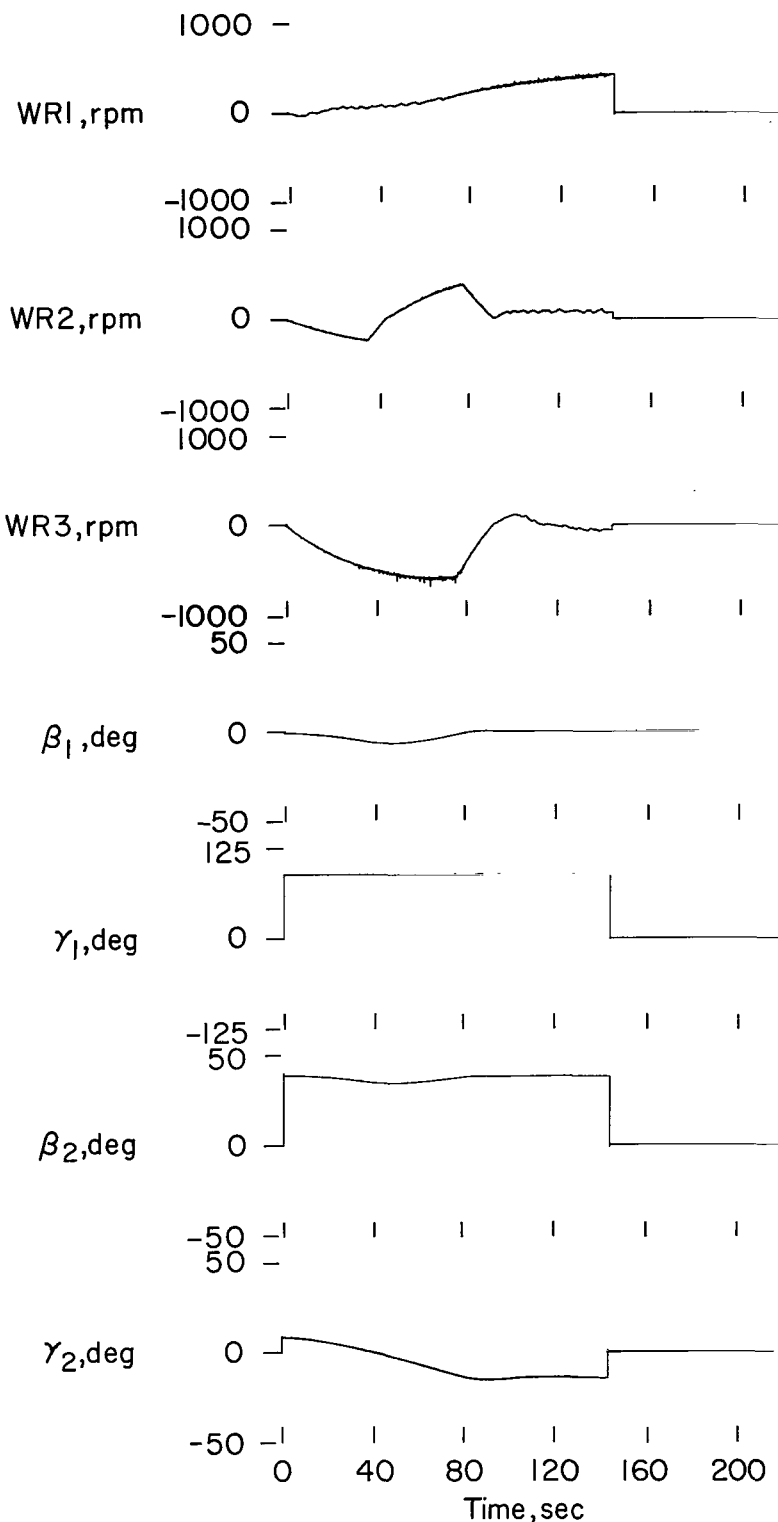


Figure 14.- Reorientation through restricted region using partial processor with zero initial momentum - Concluded.

NATIONAL AERONAUTICS AND SPACE ADMINISTRATION

WASHINGTON, D. C. 20546

OFFICIAL BUSINESS

FIRST CLASS MAIL



POSTAGE AND FEES PAID
NATIONAL AERONAUTICS AND
SPACE ADMINISTRATION

ASTER: If Undeliverable (Section 15c
Postal Manual) Do Not Retu

"The aeronautical and space activities of the United States shall be conducted so as to contribute . . . to the expansion of human knowledge of phenomena in the atmosphere and space. The Administration shall provide for the widest practicable and appropriate dissemination of information concerning its activities and the results thereof."

— NATIONAL AERONAUTICS AND SPACE ACT OF 1958

NASA SCIENTIFIC AND TECHNICAL PUBLICATIONS

TECHNICAL REPORTS: Scientific and technical information considered important, complete, and a lasting contribution to existing knowledge.

TECHNICAL NOTES: Information less broad in scope but nevertheless of importance as a contribution to existing knowledge.

TECHNICAL MEMORANDUMS: Information receiving limited distribution because of preliminary data, security classification, or other reasons.

CONTRACTOR REPORTS: Scientific and technical information generated under a NASA contract or grant and considered an important contribution to existing knowledge.

TECHNICAL TRANSLATIONS: Information published in a foreign language considered to merit NASA distribution in English.

SPECIAL PUBLICATIONS: Information derived from or of value to NASA activities. Publications include conference proceedings, monographs, data compilations, handbooks, sourcebooks, and special bibliographies.

TECHNOLOGY UTILIZATION

PUBLICATIONS: Information on technology used by NASA that may be of particular interest in commercial and other non-aerospace applications. Publications include Tech Briefs, Technology Utilization Reports and Notes, and Technology Surveys.

Details on the availability of these publications may be obtained from:

SCIENTIFIC AND TECHNICAL INFORMATION DIVISION

NATIONAL AERONAUTICS AND SPACE ADMINISTRATION

Washington, D.C. 20546